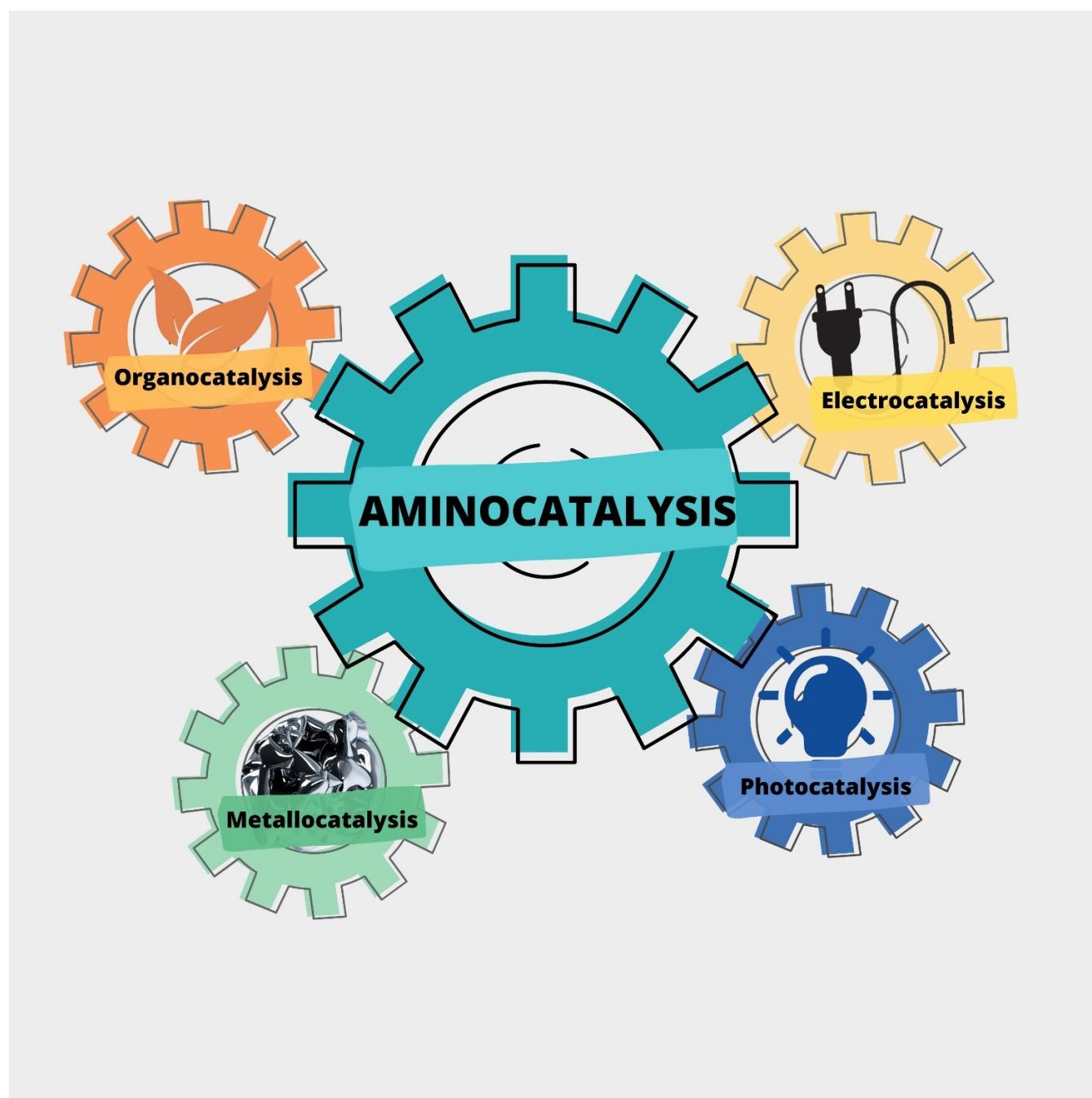


# Synergistic Strategies in Aminocatalysis

Antonio Del Vecchio<sup>+, [a]</sup> Arianna Sinibaldi<sup>+, [a]</sup> Valeria Nori,<sup>[a]</sup> Giuliana Giorgianni,<sup>[a]</sup>  
Graziano Di Carmine,<sup>[b]</sup> and Fabio Pesciaoli<sup>\*[a]</sup>



**Abstract:** Synergistic catalysis offers the unique possibility of simultaneous activation of both the nucleophile and the electrophile in a reaction. A requirement for this strategy is the stability of the active species towards the reaction conditions and the two concerted catalytic cycles. Since the beginning of the century, aminocatalysis has been established as a platform for the stereoselective activation of carbonyl compounds through HOMO-raising or LUMO-lowering. The

burgeoning era of aminocatalysis has been driven by a deep understanding of these activation and stereinduction modes, thanks to the introduction of versatile and privileged chiral amines. The aim of this review is to cover recent developments in synergistic strategies involving aminocatalysis in combination with organo-, metal-, photo-, and electrocatalysis, focusing on the evolution of privileged aminocatalysts architectures.

## 1. Introduction

Since the re-discovery of its terrific potential in 2000s, aminocatalysis has set the stage for the enantioselective functionalization of carbonyl compounds through HOMO-raising and LUMO-lowering activation. List and MacMillan's groups generalized the above-mentioned concept for the  $\alpha$ - and  $\beta$ -functionalization of aldehydes.<sup>[1]</sup> For the last 20 years aminocatalysis has been applied to a tremendous array of transformations, in the presence of electrophilic and nucleophilic species, to forge single C–C or C–X bonds or for the design of elegant tandem or cascade reactions for the construction of complex structures in one step.<sup>[2]</sup> The “gold-rush on aminocatalysis”<sup>[29]</sup> was also made possible by the introduction of privileged secondary and primary amine catalysts together with a deep understanding of their mechanism of action (Figure 1).

In Figure 1 the HOMO-raising  $\alpha$  to  $\varepsilon$  activation modes and  $\beta$  and  $\gamma$  functionalization through LUMO-lowering are highlighted. Once the potentialities and the mildness of this catalytic platform were understood, aminocatalysis gained an impressive traction ranging from single bond formation to synergistic combination with other synthetic strategies. The aminocatalytic activation of carbonyl compounds opened up the path for several enantioselective transformations. This research area can be divided into two main parts: HOMO-raising and LUMO-lowering activation. In synergistic combination with other activation platforms, in most cases, the stereoselective carbonyl compounds activation is addressed by the chiral amine catalysts. The other catalyst operates simultaneously on

the energy of the frontier molecular orbital of the reaction partner.<sup>[3]</sup>

These concurrent activations originate two reactive species, one with a higher HOMO and the other with a lower LUMO, in comparison to the respective unactivated starting materials (Figure 2).

As consequence, the energy gap between HOMO and LUMO decreases, allowing previously unattainable reactions to take place or improving the efficiency and the selectivity of existing monocatalytic transformations. However, this cutting-edge strategy is extremely challenging: the two catalytic species could easily undergo to self-quenching, rendering the synthetic strategy inefficient. In fact, on synergistic catalysis involving aminocatalysis it is necessary to carefully tune the reaction conditions in order to avoid catalysts annihilation. In other cases, a completely new catalyst is required to overcome this problem. The aim of this review is to discuss the recent development of synergistic aminocatalysis, and its synergistic combination with other synthetic platforms, from 2015. Through the four sections, a critical overview of the most common synergistic systems involving amino-organo, amino-metal, amino-photoredox and amino-electrocatalysis will be provided. Finally, some selected examples of differentiating catalysis are also included. In stark contrast with synergistic catalysis, in this strategy two molecules of a single catalyst activate both the electrophile and the nucleophile through two catalytic cycles that work synergistically.

[a] Dr. A. Del Vecchio,<sup>+</sup> A. Sinibaldi,<sup>+</sup> V. Nori, G. Giorgianni, Dr. F. Pescioli  
Department of Physical and Chemical Sciences  
Università degli Studi dell'Aquila  
via Vetoio, 67100, L'Aquila (Italy)  
E-mail: fabio.pescioli@univaq.it

[b] Dr. G. Di Carmine  
Department of Chemical, Pharmaceutical and  
Agricultural Sciences Università degli Studi di Ferrara  
Via Fossato di Mortara 17, 44121,  
Ferrara (Italy)

[<sup>+</sup>] These authors contributed equally to this work

© 2022 The Authors. Chemistry - A European Journal published by Wiley-VCH GmbH. This is an open access article under the terms of the Creative Commons Attribution Non-Commercial NoDerivs License, which permits use and distribution in any medium, provided the original work is properly cited, the use is non-commercial and no modifications or adaptations are made.

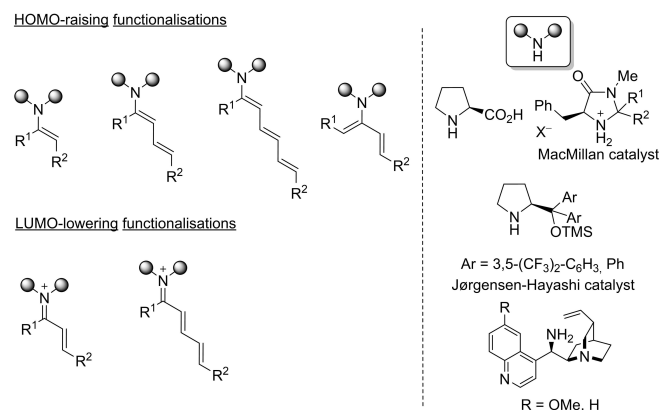
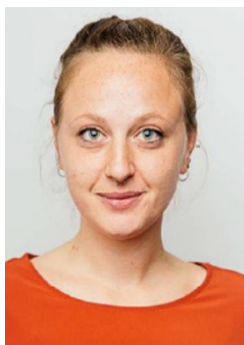


**Figure 1.** Principal activation modes and privileged catalysts in aminocatalysis.

Antonio Del Vecchio obtained his MSc in chemistry and pharmaceutical technologies at the University of Ferrara (Italy). In 2016, he joined the Service de Chimie Bioorthogonale et de Marquage (SCBM) at the CEA in Saclay where he received his Ph.D. on new synthetic methodologies involving CO<sub>2</sub> and carbon radiolabeling under the supervision of Drs. Davide Audisio and Frédéric Taran. From 2019 to 2021, he was a postdoctoral researcher in Prof. Dr. Ackermann's group at the Georg-August-Universität Göttingen (Germany) working on metalla-electrocatalyzed C–H activations before briefly joining Prof. Carlone's group as a research associate. In September 2021, he started work as a postdoctoral researcher in Dr. Mauduit group at the Organometallic Chemistry Department at Ecole Nationale Supérieure de Rennes.



In 2017, Arianna Sinibaldi obtained her master's degree in biomolecular and organic chemistry at "La Sapienza-Università di Roma" under the supervision of Prof. Marco Bella. After graduation, she won a Regione Lazio (Torno Subito-Work Experiences) scholarship to spend six months in the group of Prof. Andrei Malkov at Loughborough University (UK) before continuing her research at "La Sapienza" for five more months. Since November 2018, she has been a PhD candidate under the supervision of Prof. Armando Carlone. She focuses on supramolecular aminocatalysis and innovative activation modes for more efficient organocatalysis.



Valeria Nori obtained her master's degree with honors in chemical sciences at the Università degli Studi dell'Aquila in 2018 and is currently in the final year of her PhD. She focuses on the study of catalytic methods by means of organocatalysis, metal catalysis and synergistic catalysis, towards pharmaceutically interesting fragments. From September 2019 to April 2020, she was a visiting PhD candidate in the laboratory of Dr Rebecca Melen at Cardiff University (UK) developing skills in the field of boron catalysis.



Giuliana Giorgianni obtained her M. Sc. with honors in chemical sciences at the Università degli Studi dell'Aquila under the supervision of Armando Carlone in 2019. In 2020 she started a PON industrial PhD funded by the EU, under the supervision of Armando Carlone. During the first year of her PhD, she worked at the Università degli studi dell'Aquila, in the field of organocatalysis. In 2021 she spent 10 months at the University of Vienna in the Bonifazi group, where she worked on intramolecular photocyclizations of aromatic polycyclic systems. She is currently spending 6 months at F.I.S. in Vicenza.



Graziano Di Carmine obtained bachelor's and master's degrees in chemistry at the Universities of Rome "Tor Vergata" and Bologna, respectively. In 2019, he obtained a PhD in chemistry at the University of Ferrara under the supervision of Prof. Olga Bortolini, working on the umpolung reactivity promoted by enzymatic- and organo-catalysis. He was a Research Fellow at ISOF CNR of Bologna and Research Associate at University of Manchester, where he worked on immobilization of organocatalysts and relaxation measurements in NMR spectroscopy for mechanistic studies in heterogeneous organocatalysis, respectively. In 2020 he was appointed as fixed-term researcher (RTDa) at the University of Ferrara, working on homogeneous and heterogeneous organocatalysis, and photocatalysis.



Fabio Pesciaoli earned his PhD in chemical sciences in 2011 under the supervision of Profs. Giuseppe Bartoli and Paolo Melchiorre focusing on asymmetric aminocatalysis. In 2011, as a postdoc in Prof. Dr Benjamin List's group at the Max Planck Institut für Kohlenforschung, he started work on Brønsted and Lewis acid-based organocatalysis. After a stay as a Cariplo Fellow at Pavia University in the group of Prof. Zanoni, he joined Prof. Lutz Ackermann's group at Göttingen University focusing mainly on asymmetric C–H activation by using catalytic amounts of 3d transition metal based catalysts. In 2020, he was appointed as fixed-term researcher (RTDa) at the Università degli Studi dell'Aquila, working on organocatalytic eco-friendly transformations and C–H activation.



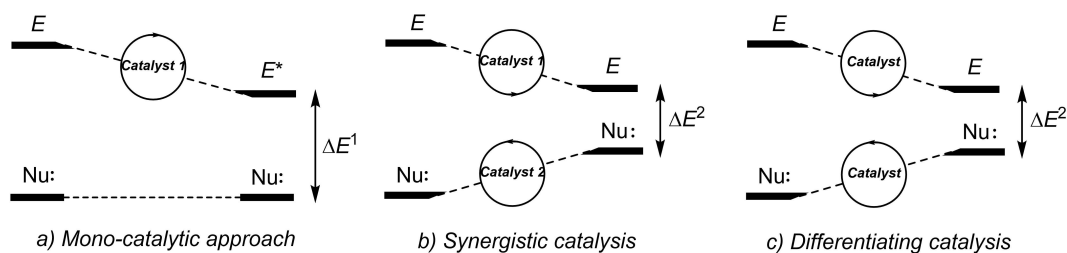


Figure 2. Comparison between the monocatalytic approach (LUMO-lowering), synergistic catalysis, and differentiating catalysis.

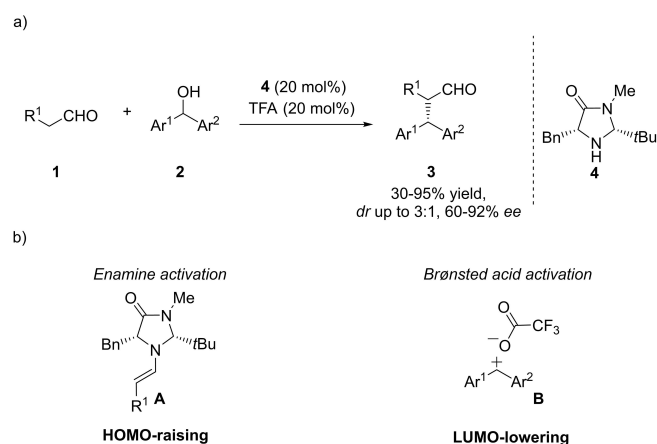
## 2. Amino-organo Synergistic Catalysis

### 2.1. General aspects

Amino-organo synergistic catalysis became a pivotal research area for enantioselective  $\alpha$  C–C bond formation by enamine catalysis, challenging as well intermolecular  $\alpha$ -alkylation, a long-standing synthetic problem.<sup>[4]</sup> HOMO-raising activation was also applied to the development of synergistic Diels-Alder reactions. LUMO-lowering activation was applied to the design of synergistic [3+2] cycloaddition and Michael addition to  $\alpha,\beta$ -unsaturated carbonyl compounds.

### 2.2. Early work

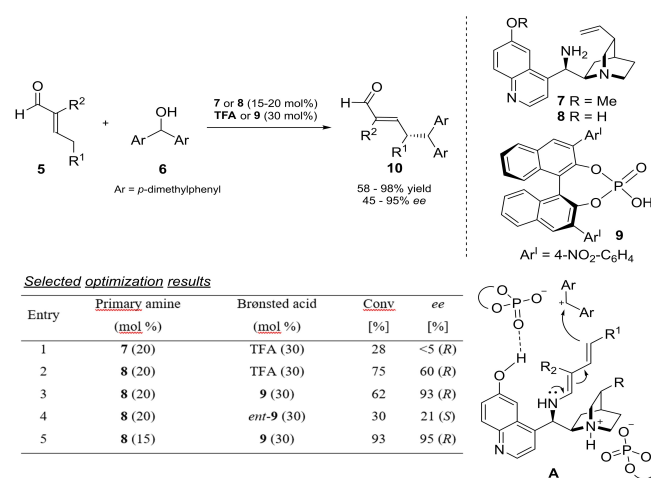
Driven by the pioneering contributions of List<sup>[1a]</sup> and MacMillan,<sup>[1b]</sup> the intensive studies of aminocatalytic carbonyl activation, emphasized the role of a Brønsted acidic functional group or co-catalyst able to accelerate the formation and the hydrolysis of the reactive intermediates in the catalytic cycle. In this perspective, Cozzi et al. demonstrated in 2009 the possibility of employing an achiral Brønsted acid in combination with the MacMillan imidazolidinone **4**, for a highly enantioselective synergistic enamine/Brønsted acid  $\alpha$ -alkylation of aldehydes (Scheme 1a).<sup>[5]</sup>



Scheme 1.  $\alpha$ -Alkylation of aldehydes by synergistic amino/Brønsted acid catalysis.

Macmillan imidazolidinone activates the aldehyde **1** through HOMO-raising enamine formation **A**, while TFA promotes the LUMO-lowering of **2** through the formation of carbocation **B** (Scheme 1b). The carbocation pathway is supported by the reaction carried out with enantiopure (*S*)-ferrocenyl(phenyl)methanol that arises the product in high enantiomeric excess but with 3 to 1 diastomeric ratio. In 2010, Melchiorre et al. extended this strategy to the  $\gamma$ -functionalization of  $\alpha$ -branched enals employing a bifunctional primary amine **8** and a BINOL-based chiral phosphoric acid **9**, achieving outstanding stereoselectivities (Scheme 2).<sup>[6]</sup>

The optimization points out the key role of both the chiral amine **8** and the chiral Brønsted acid **9**. Carrying out the reaction with the 9-amino(9-deoxy)*epi* quinidine **7** in presence of TFA resulted into poor conversion and no enantio-induction (entry 1). In sharp contrast, the easily accessible amine **8** engages the Brønsted acid with the free hydroxy group ensuring a high structured transition state **A** (entry 2). The use of a matching chiral enantiopure acid **9** in two to one ratio respect to **8** is essential for achieving outstanding results (entries 3–5), underlining the double role of **9** as counter-anion of the benzydril cation and the quinuclidine ammonium salt. This enamine/Brønsted acid synergistic catalysis results in several contributions over the years,<sup>[7]</sup> being also applied to the



Scheme 2.  $\gamma$ -Alkylation of  $\alpha$ -branched enals by synergistic amino/Brønsted acid catalysis.

total synthesis of (+)-gliocladin C in 12 steps and 19% overall yield.<sup>[8]</sup>

### 2.3. Enamine-organo synergistic catalysis

In 2015, Wang et al. envisaged the synergistic enamine/Brønsted acid addition of aldehydes to 4-vinyl pyridine **11**. The reaction required a judicious optimization. Weak acids were unable to activate the vinyl pyridine through LUMO-lowering by means of protonation of the heterocyclic nitrogen, while the choice of TfOH resulted optimal. Interestingly, commercially available OTMS-protected Jørgensen/Hayashi catalyst afforded the desired product in poor enantiomeric excess. The choice of bulkier silyl protected diphenyl prolinol catalyst **13** together with the use of DMF:H<sub>2</sub>O (8:2) solvent system, ensured high stereoselectivities (Scheme 3a).<sup>[9]</sup>

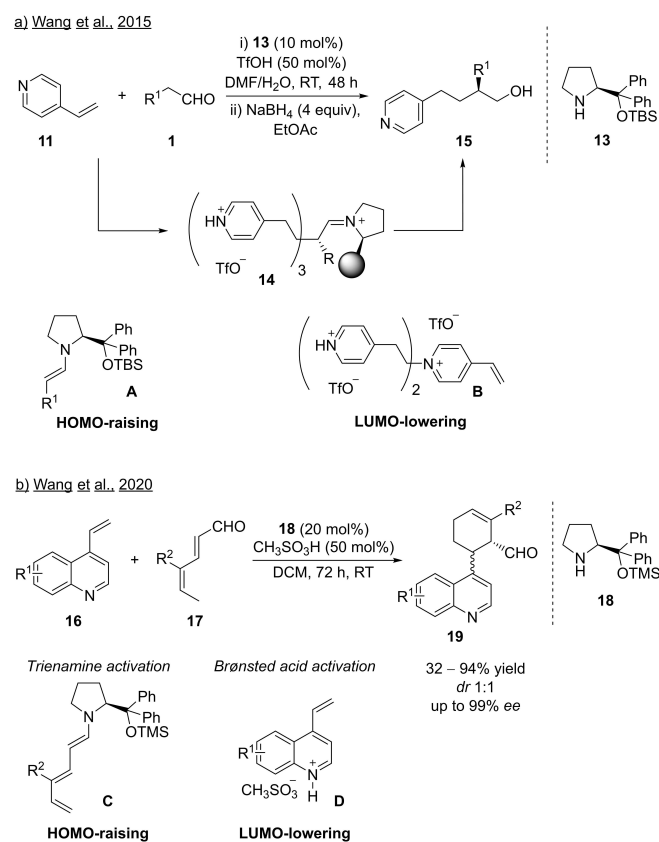
In this reaction (Scheme 3a), amino-catalyst **13** promotes the HOMO-raising of the carbonyl compound **1**; regarding the LUMO-lowering of **11**, the actual electrophile that undergoes the enamine attack is a protonated trimeric 4-vinylpyridinium species **B**. After the enantioselective attack, the product is formed upon the depolymerization of intermediate **14** and the iminium ion hydrolysis. Relying on chiral amine catalyzed trienamine formation **C** (Figure 1), Wang's group extended its

synergistic activation strategy on the [4+2] cycloaddition of dienals and 2- and 4-vinyl-quinolines **16**, through trienamine/Brønsted acid synergistic activation (Scheme 3b).<sup>[10]</sup> The reaction afforded 4-functionalised quinoline **19** in excellent yield and enantiomeric excess as a mixture of diastereoisomers. Contrary to the previous report (Scheme 3a), trimeric protonated vinyl arene species were not observed, indeed the LUMO-lowering of the electrophile was ensured by the formation of the intermediate **D**. Recently, Chen group has applied the trienamine catalyzed [4+2] cycloaddition of dienals **20** on the *ortho*-formyl cinnamates **21** by differentiating double amino catalysis (Scheme 4).<sup>[11]</sup>

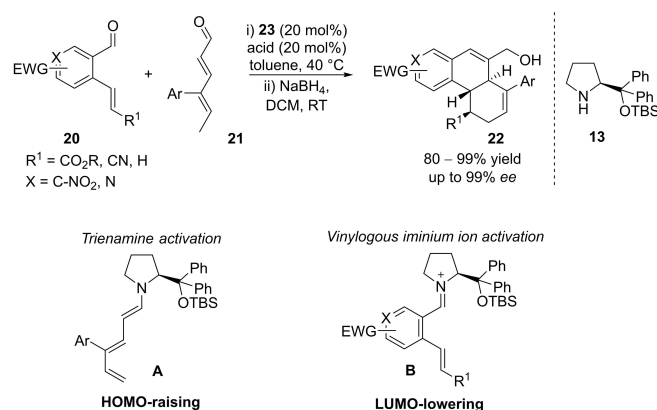
The reported Diels–Alder/aldol condensation tandem reaction allows the construction of polycyclic motifs **22** as a single diastereoisomer in high yield and excellent enantiomeric excess when cinnamates are used as dienophiles. In case of *ortho*-formyl styrene (R<sup>1</sup> = H) the diastereoselectivity decreases to 3:1 while maintaining excellent *ee*. Jørgensen/Hayashi catalyst **13** activates both the partners of the reaction through trienamine formation (**A**) and lowering the LUMO of the remote dienophile via an iminium ion (**B**).

Merging HOMO-raising activation by enamine with boronic acid catalysis, Hall et al. reported the allylation of  $\alpha$ -branched aldehydes through the formation of a stabilized carbocation (Scheme 5a).<sup>[12]</sup> In this reaction, the intermediate **B** generated by the ferrocenyl boronic acid catalyst **25** and the alcohol **24**, is engaged by the chiral enamine **E**, providing the  $\alpha$ -allylated phenyl propanals **23** (R<sup>1</sup> = Me) in good yields and excellent stereoselectivities. Bulkier substrates (R<sup>1</sup> = Et) undergo sluggish reactions (19% yield, 60% *ee*).

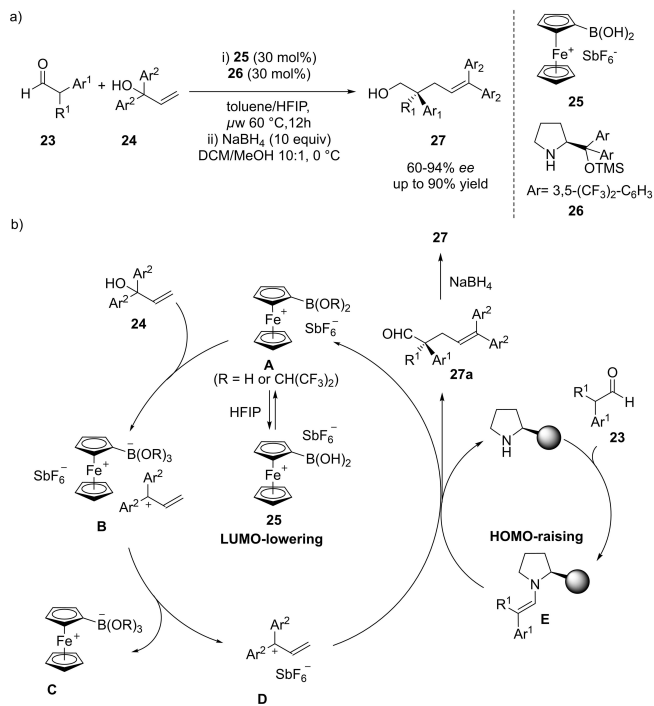
The choice of amino-catalyst **26** resulted crucial, since the more basic *gem*-diphenyl analogue **18** was unable to catalyze the reaction, undergoing annihilation presumably with the Lewis acid **25** or other Lewis acidic species present in the reaction. While the enamine catalytic cycle promotes the HOMO-raising of the aldehyde **23**, the LUMO-lowering of the allyl alcohol **24** is more complex and it warrants further discussions (Scheme 5b). It was hypothesized that the actual Lewis acid catalyst is the Boronic acid bis-(hexafluoroisoprop-



**Scheme 3.** a) Synergistic enamine/Brønsted acid-catalyzed  $\alpha$ -addition of 4-vinyl pyridines to aldehydes. b) Formal [4+2] cycloaddition of dienals to 4-vinyl quinolines.



**Scheme 4.** Trienamine-catalyzed [4+2] cycloaddition of dienals on *ortho*-formyl cinnamates.



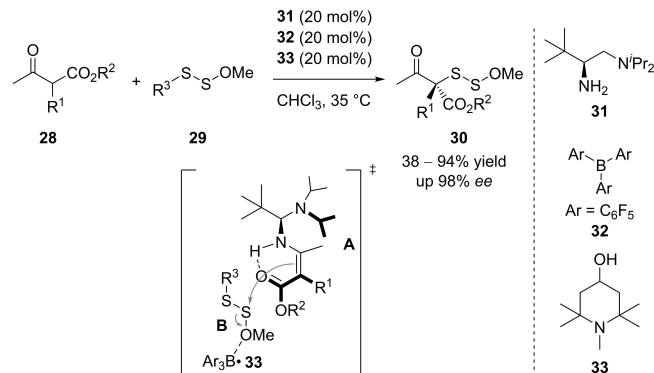
**Scheme 5.** Allylation of  $\alpha$ -branched aldehydes through synergistic enamine/Lewis acid catalysis.

oxide) **A** that is formed in situ by a dynamic equilibrium with **25** in presence of HFIP. The above-mentioned active species, generates the carbocation intermediate **B** in presence of **24**, that subsequently undergoes an anion exchange to form the carbocation hexafluoroantimonate **D**. This activated intermediate is stereoselectively intercepted by the enamine **E**, which attacks the electrophile **23** with subsequent release of the product **28** (Scheme 5b). Recently, relying on HOMO-raising/frustrated Lewis pair (FLP) synergistic catalysis, Luo et al. performed the  $\alpha$ -disulfuration of  $\alpha$ -branched keto-esters **28**. Primary-tertiary amine catalyst **31**, already successfully employed for other non-synergistic transformations involving highly sterically demanding carbonyl compounds,<sup>[13]</sup> afforded **30** in good yields and excellent ee (Scheme 6).<sup>[14]</sup>

Interestingly, catalytic amounts of the external tertiary amine **33** resulted as well crucial, improving both the yield and the stereoselectivity of the reaction, while the use of TfOH instead of **32** was detrimental. In the proposed transition state, chiral amine **31** activates **28** through HOMO-raising. Triaryl borane **33** coordinates the disulfide **29** favoring the stereoselective enamine attack.

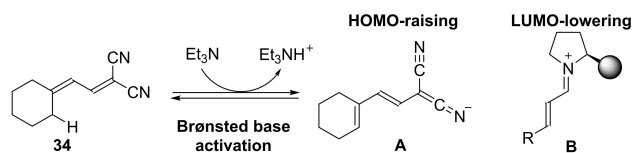
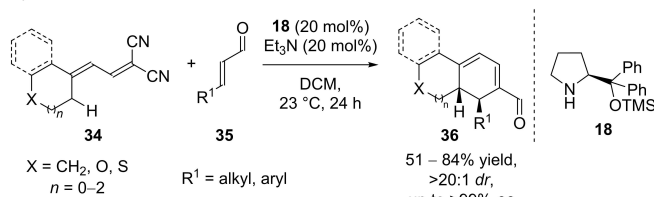
## 2.4. Iminium ion-organo synergistic catalysis

In 2015, Brønsted base catalysis was further applied synergistically with iminium ion catalysis<sup>[15]</sup> by Zanardi et al. for a formal *endo*-like [4 + 2] cycloaddition of vinylous allylidene malononitriles **34** and enals **35** employing catalyst **18** and  $\text{NEt}_3$  as a Brønsted base (Scheme 7a). The products **36** were obtained in

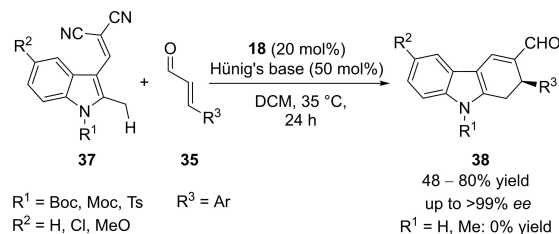


**Scheme 6.** Asymmetric disulfuration of  $\alpha$ -branched keto-esters through synergistic enamine/FLP catalysis.

### a) Zanardi, 2015



### b) Rassu and Zanardi, 2016



**Scheme 7.** a) [4 + 2] cycloaddition of vinylous malononitriles to enals by iminium ion/Brønsted base catalysis; b) [4 + 2] cycloaddition of vinylous 2-methylindolyl methyl-enemalononitriles to enals.

high yields and full control of stereoselectivity, moreover, this synergistic strategy was applied to the post-functionalization of steroidal molecules with high selectivity, regardless the configuration of the starting material. The vinylous malononitrile **34** undergoes a remote  $\epsilon$ -proton abstraction in presence of  $\text{Et}_3\text{N}$ , forming the diene **A** that intercepts the iminium ion **B**. In the stereo-determining step of the reaction, *endo*-like transition state is favoured by Coulombic interaction while catalyst **18** selectively shields the *Re* face. Subsequently, the enamine intermediate eliminates malononitrile forming an iminium ion that upon hydrolysis provides the final product **36**.

Based on this proposed mechanism, the authors also performed the reaction in presence of catalytic amount of

**Table 1.** Key optimization experiments of the [3 + 2] cycloaddition of nitrones to enals by iminium ion/Brønsted base catalysis.

**Catalysts:**

**18:**

**41:**

**Additive:**

**42:**

	Catalyst	Additive	Yield [%]	<i>dr</i>	<i>ee</i> [%]
1	<b>18</b>	none	< 5	–	–
2	<b>18</b>	PhCO <sub>2</sub> H	< 5	–	–
3	<b>18</b>	<b>42</b>	47	5:1	97
4	<b>41</b>	none	40	4:1	20
5 <sup>[a]</sup>	<b>18</b>	<b>42</b>	92	5:1	98

[a] NEt<sub>3</sub> (20 mol%) was added.

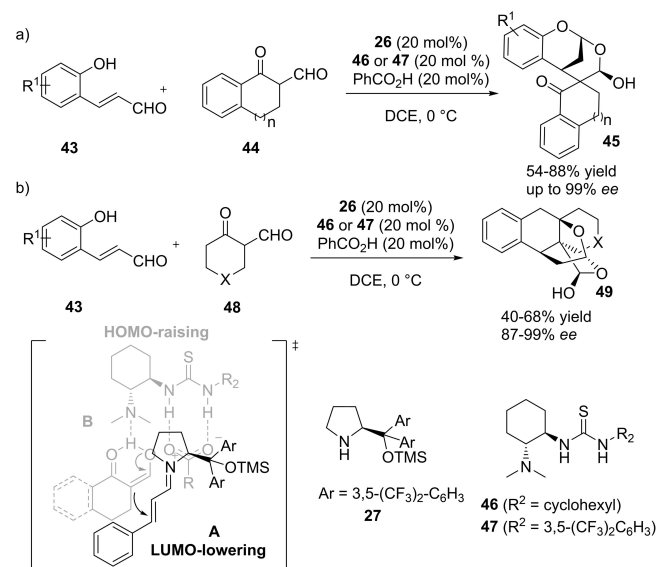
malononitrile, obtaining the product in high yield, albeit with lower enantiomeric excess. In 2016, Rassu and Zanardi applied their strategy to the stereoselective synthesis of 2,9-dihydro-1*H*-carbazoles **38** in outstanding *ee*. In this reaction, 2-methylindolyl methyl-enamalononitriles **37** intercepts the dienophile iminium ion intermediate after remote deprotonation in presence of Hünig's base (Scheme 7b).<sup>[16]</sup>

In 2017, inspired by the seminal contribution of Córdova et al.,<sup>[17]</sup> the group of Vicario developed a dipolar [3 + 2] cycloaddition reaction of  $\alpha,\beta$ -unsaturated aldehydes **35** and nitrones ylides, formed in situ from **39** upon synergistic iminium ion/hydrogen bonding catalysis. The manifold allows the construction of *N*-hydroxypyrrolidines **40** bearing four contiguous stereocenters in high yield and excellent enantioselectivity.<sup>[18]</sup>

The catalyst **18** was employed to activate enal **35** as a dipolarophile (A), controlling the facial selectivity of the process, while the Schreiner thiourea **42** results critical to raise the HOMO energy of nitrone ylides B (Table 1). During optimization studies, the authors underlined that a synergistic approach was crucial to success. Indeed, amino-catalyst **18** resulted unable to promote the formation of the [3 + 2] product as well as in presence of catalytic amounts of benzoic acid (entries 1 and 2). Thiourea **42** in quality of hydrogen-bonds donor catalyst, was essential for the ylide activation (B). It is noteworthy that the bifunctional iminium ion/H-bonding donor catalyst **41** shows lower stereocontrol compared to the synergistic system (entry 4). Triethylamine as a Brønsted base catalyst was beneficial for the reaction, enhancing the yields and the rate of the ylide formation (entries 3–5).

Moving to bifunctional chiral Brønsted base catalysis in combination with aminocatalysis, Liu et al. designed a synergistic iminium ion/Brønsted base catalysis assisted by counter anion binding, through quinary catalyst-substrate systems.<sup>[19]</sup> The substrate-controlled reaction afforded bridged or cage-like polyheterocyclic compounds **45–49** (Scheme 8).

Submitting 2-hydroxycinnamaldehydes **43** and benzofused cyclic  $\beta$ -oxo aldehydes **44** in presence of catalytic amount of

**Scheme 8.** Synergistic iminium ion/Brønsted base catalysis assisted by counter-anion binding.

Takemoto catalyst **46** (or **47**), and amine **27** as benzoate salt, resulted into the formation of a single stereoisomer of the final product **45** in high yield (Scheme 8a). On the other hand, in presence of simple cyclic  $\beta$ -oxo aldehydes **48**, the synergistic catalytic protocol afforded cage-like polyheterocyclic products **49** (Scheme 8b).

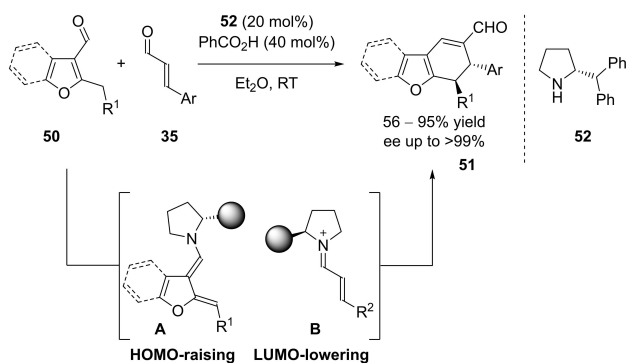
From a mechanistic point of view, the outstanding stereoselectivities achieved in the transformation reflect the high organization of the transition state. The tertiary amine moiety of the Takemoto catalyst **46** or **47** ensures the HOMO-raising activation of  $\beta$ -oxo aldehyde **44–48** (**B**). The  $\alpha$ ,  $\beta$ -unsaturated aldehyde **43** is activated through LUMO-lowering by the secondary amine catalyst. The counter-anion of this intermediate is binded by the thiourea moiety of **46** or **47**, allowing the facial control through an electrostatic interaction.

Based on those results, the authors could further report the synthesis of two other classes of benzofused bicyclo[3.3.1] nonane scaffolds.<sup>[20]</sup>

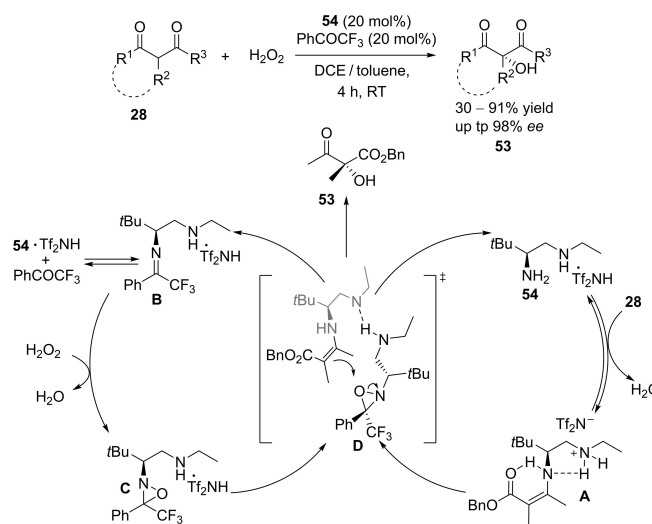
Aminocatalysts possess the ability to promote HOMO-raising LUMO-lowering activation depending on the substrate. Building up on this feature, the scientific community designed several tandem and cascade reactions. On the other hand, the synergistic activation of both reaction partners by two molecules of the same catalyst, called differentiating catalysis, represents an appealing and relatively unexplored synthetic strategy.<sup>[21]</sup> Recently, Albrecht et al. applied this concepts to the asymmetric [4 + 2] cycloaddition  $\beta$ -enals **35** and 2-alkyl-3-formylheteroarenes **50** (Scheme 9).<sup>[22]</sup>

Cycloadducts **51** are forged in outstanding stereoselectivities upon reaction with **52** that has a dichotomous role: it catalyzes the dearomatization of **50** through dienamine formation and it activates the dienophile **35** through iminium ion formation. In 2021, Luo et al. designed an elegant  $\alpha$ -oxidation of  $\beta$ -ketoester **28** relying also on differentiating catalysis. The authors applied this strategy in an enamine/carbonyl synergistic transformation achieving the desired oxygenated product **53**, providing a quaternary stereocenter in excellent enantioselectivities (Scheme 10).<sup>[23]</sup>

The authors proposed a differentiating catalytic system where the chiral primary amine **54** is involved in both the HOMO-raising activation of the encumbered carbonyl compound and in the activation of the oxidant. In particular, kinetic



**Scheme 9.** Differentiating catalysis in [4 + 2] cycloaddition.



**Scheme 10.** Synergistic chiral amine/ketone catalysis for the  $\alpha$ -oxygenation of encumbered carbonyl compounds.

and DFT studies support H<sub>2</sub>O<sub>2</sub> activation through oxaziridine **C** formation, generated by the condensation between trifluoroacetophenone and **54**. This intermediate is then intercepted by the enamine **A** in a highly stereoselective fashion (**D**). The authors further support this reaction mechanism by observing a negative non-linear effect that suggests the presence of two molecules of the chiral amine **54** in the enantiodetermining step.

The synergistic combination of well-established organocatalytic strategies with aminocatalysis, allowed to expand the potentialities of this synthetic toolbox towards transformations that were not accessible before. Moreover, the combination of commercially available catalysts despite bifunctional chiral ones, offers the possibility of tuning accurately the activation pathways of both substrates, without addressing long multi-steps syntheses. On the other hand, synergistic amino-organocatalysis still relies on high catalytic loadings that hamper its application in an industrial scenario. In this context, the use of heterogeneous and recyclable organocatalysts might represent a promising alternative.

## 3. Amino-metal Synergistic Catalysis

### 3.1. General aspects

The synergy between amino and metal catalysis, in particular transition metal catalysis, reverts a strategic role for the development of asymmetric transformations. The combination and the co-existence of two distinct catalytic systems able to complete each other, furnishes an effective manifold for a simultaneous HOMO-raising/LUMO-lowering of the involved species.<sup>[24]</sup> Finally, it is worth mentioning the tremendous developments achieved in the field of synergistic aminocatalysis in presence of Lewis acids. However, since the argument has been already extensively treated by other reviews,<sup>[25]</sup> in the next



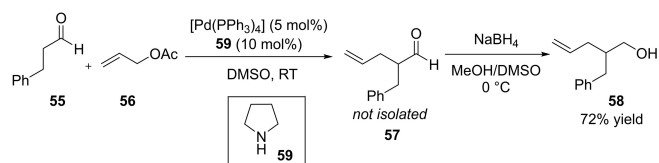
section the synergistic catalysis between amines and noble metals will be preferentially discussed.

### 3.2. Early work

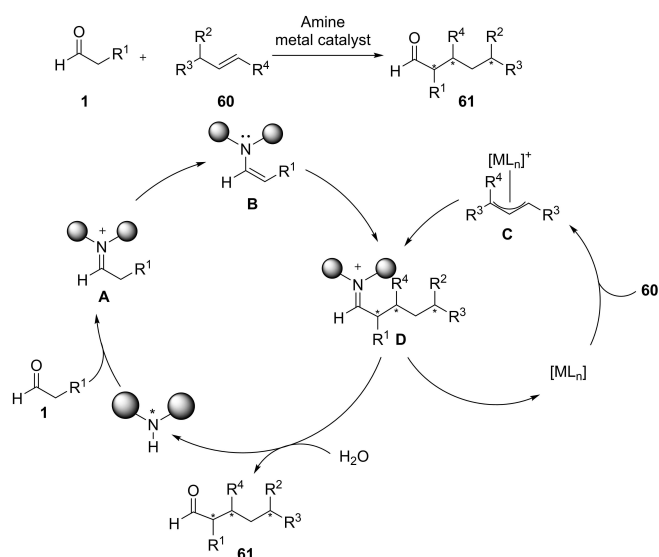
The group of Cordova proved the efficacy of combining metal and amino catalysis for the  $\alpha$ -alkylation of aldehydes **55** (Scheme 11).<sup>[26]</sup>

Reacting the aldehyde **55** in presence of allyl acetate **56** [Pd(PPh<sub>3</sub>)<sub>4</sub>] and pyrrolidine **59**, the corresponding branched product could be isolated with 72% yield upon reduction from the aldehyde **57**. The synergistic metal-enamine approach for the enantioselective functionalization of aldehydes and ketones is generally hypothesized to occur through a precise mechanism, involving the in-situ formation of chiral iminium ion **A** followed by tautomerization to the enamine **B**. Such nucleophilic species is then able to react with the corresponding electrophile **C**: a metalated species formed at the same time upon reaction between metal and allyl moieties **60**. The following hydrolysis of **D** allows the release of the desired product **61**. The enantioselectivity is guaranteed both by the chiral enantiopure amino-catalyst and metal ligands (Scheme 12).

In 2007, Carreira and co-workers reported the combination of iridium and the phosphoramidite ligand (*rac*)-**65** to promote the formation of an allyl-ammonium compound **64**. The



Scheme 11. Synergistic enamine/Pd<sup>0</sup>  $\alpha$ -alkylation of aldehydes.



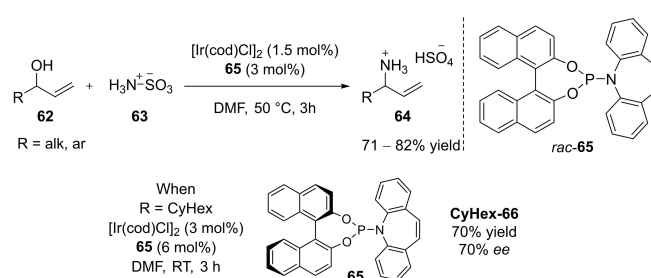
Scheme 12. General mechanism for amino-metal synergistic catalysis.

employment of **65** led to the formation of the allylation product CyHex-**66** with the control of stereoselectivity (Scheme 13).<sup>[27]</sup>

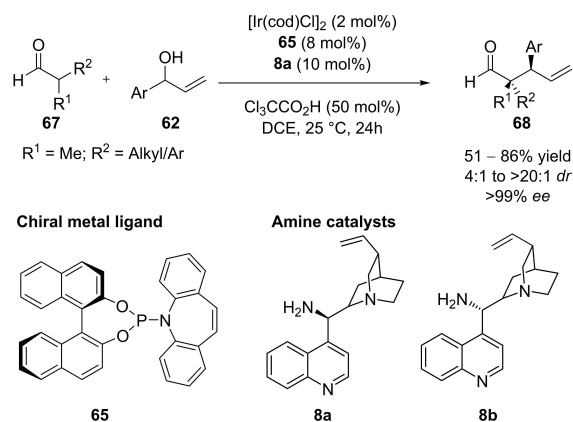
### 3.3. Enamine-metal synergistic catalysis

Given these observations, in 2013 Carreira's group developed a method for a synergistic Ir-enamine-catalyzed stereoselective functionalization of carbonyl moieties in presence of allyl-alcohols **62**. Also in this case, chiral phosphoramidite ligand **65** ensues the stereoselection on the olefin coordination by the iridium complex. The *Cinchona* alkaloid-derived primary amine **8a** could react with the aldehyde **67**, leading to the formation of a chiral enamine, able to react with the Ir-allyl intermediate. The mild reaction conditions allowed the formation of the desired allylation products **68**. Within isolated yields ranging from 51% if a strong EDG is present on the aromatic ring as substituent of the allylic alcohol, to 86% for the model substrates. Branched aldehydes showed a lower reactivity compared to the model. In all cases, the enantioselectivities observed were excellent (>99%). Additionally, the catalyst permutation could lead to the preparation of all the stereoisomers of the product within the same stereoselectivities. With the established procedure, a broad series of  $\alpha$ -disubstituted chiral vinyl aldehydes could be accessed (Scheme 14).<sup>[28]</sup>

One year later, the scope could be expanded with a stereoselective functionalization of linear aliphatic aldehydes



Scheme 13. Synthesis of allyl-ammonium salts.

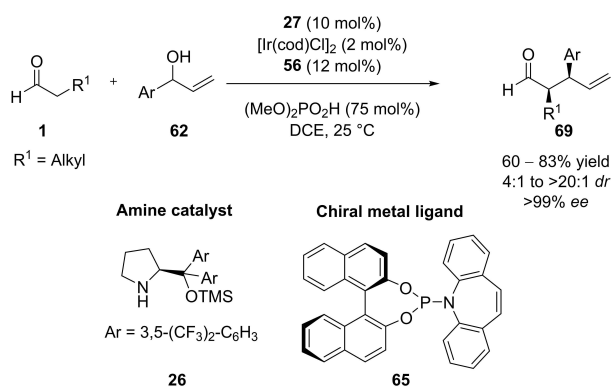


Scheme 14. Enantioselective synthesis of  $\alpha$ -disubstituted chiral vinyl aldehydes.

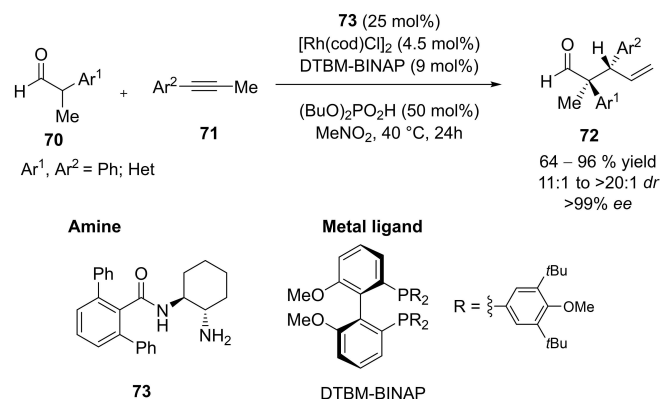
1.<sup>[29]</sup> The easily enolizable stereogenic center renders these structures passive of epimerization. This time, a derivative of the Jørgensen catalyst **26** could be efficiently employed, being able to furnish the competent chiral enamine intermediate, able to intercept the chiral **65**-Ir-allyl intermediate, generated from **62**. To reduce the enolization, a series of acidic additives were tested. Among those, dimethylhydrogen phosphate was found to be the best choice to provide **69**, being unable to influence the stereoselectivity and showing at the same time the best diastereoselectivity (20:1; Scheme 15).

Analogously, the use of chiral phosphoramidite ligand **65** and Jørgensen/Hayashi catalyst **26** favors the development of a stereodivergent procedure for the preparation of  $\alpha$ -amino and hydroxy aldehydes.<sup>[30]</sup>

In 2017, Dong proposed an alternative strategy for the enantio- and diastereoselective synthesis of vinyl aldehydes, exploiting the synergistic catalysis of rhodium and enamine for the coupling between  $\alpha$ -branched aldehydes **70** and alkynes **71**. Key point of the transformation is the in-situ generation of an electrophilic Rh–H  $\pi$ -allyl complex, trapped by the enamine intermediate, formed upon reaction between chiral amine catalyst and the aldehyde, providing access to  $\gamma,\delta$ -unsaturated aldehydes **72**. By increasing the bulkiness of the phosphine



**Scheme 15.** Enantioselective functionalization of linear aldehydes with an enolizable proton.

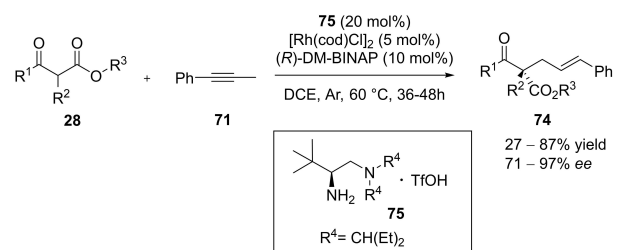


**Scheme 16.**  $\alpha$ -Alkylation of aldehydes with simple alkynes.

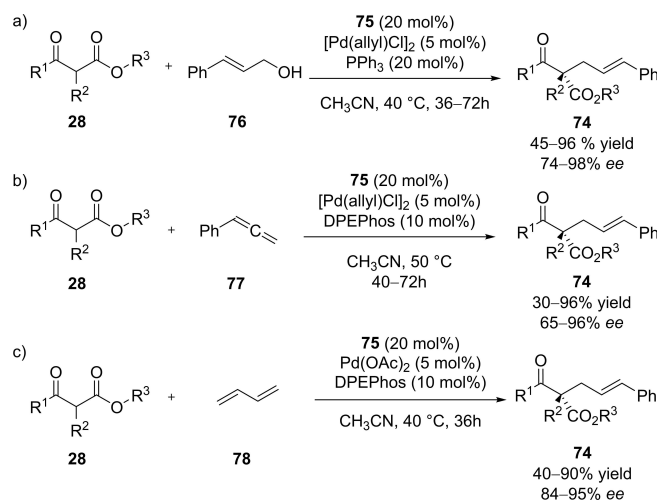
ligand and using the chiral diamines **73** high enantio and diastereoselectivities could be achieved (Scheme 16).<sup>[31]</sup>

Luo and co-workers developed an alternative strategy for the enantioselective functionalization of sterically demanding  $\alpha$ -branched-dicarbonyl derivatives **28** through the in-situ formation of a chiral enamine from the reaction with amine **75** and encumbered  $\beta$ -keto-esters.<sup>[32]</sup> The reaction, proceeding analogously to the previous report from Dong, involves also the use of the chiral ligand (*R*)-DM-Binap for the formation of a chiral Rh metallacycle. Transformation with **71** could provide the desired product **74** with yields from 27 to 86% and enantioselectivities from 71 to 95% (Scheme 17).<sup>[33]</sup>

A palladium-catalyzed procedure for the asymmetric allylic alkylation of acyclic  $\beta$ -ketoesters **28** was introduced by Luo and co-workers. For the procedure, allylic alcohols **76** were employed for the first time in asymmetric fashion. The problems related to such substrates are due to their sluggish metalation step, requiring harsher conditions to form the  $\pi$ -allyl intermediate. Under the optimized conditions, tert-butyl-2-methyl-3-oxobutanoate could be reacted with cinnamyl alcohol **76** in presence of  $\text{Pd(allyl)}_2$  and amines **31** and **75** (20 mol%) for 36 either 72 h at 40 °C, providing the corresponding allylation product **74** with isolated yields ranging from 45 to 96% and 74 to 98% enantiomeric excess (Scheme 18a).<sup>[34]</sup>



**Scheme 17.** Primary amine/Rh synergistic asymmetric catalysis for the allylation of  $\alpha$ -branched ketones.

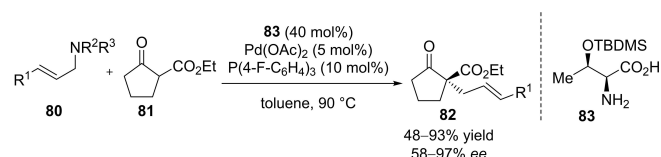


**Scheme 18.** Synergistic strategies for the  $\alpha$ -allylation of encumbered carbonyl compounds.

Inspired by the work of Dixon<sup>[35]</sup> on the synergistic amine-Pd catalysis for the intramolecular reaction between carbonyl groups and allenes, in 2016 Gonzàles<sup>[36]</sup> and Lòpez<sup>[37]</sup> reported independently an intermolecular strategy based on synergistic amine/gold catalysis, employing in a similar manner chiral enantiopure proline derivatives for the in-situ generation of the enamine and an electron-rich phosphine ligand. The reaction was proven to be efficient in presence of allenamides, providing the corresponding products in high yields. One year later, the group of Luo<sup>[38]</sup> established a protocol for the intermolecular addition of allenes **77** to dicarbonyl derivatives **28**, able to provide the desired products **74** with yields ranging from 30 to 96% and enantioselectivities from 65 to 96% (Scheme 18b). The enantiodetermining-step, alongside the in-situ formation of the chiral enamine from the reaction between **28** and the amine **75**, was the formation of  $\pi$ -allylic palladium intermediate upon hydrometallation of the allene **77**. Satisfying results could also be obtained in presence of  $\alpha$ -branched aldehydes, albeit with the achievement of slightly lower enantioselectivities (83 and 85%) using the established conditions.

In 2021, the same group, inspired by the early developments from Hartwig et al.,<sup>[39]</sup> established a procedure for the functionalization of **28** with butadiene derivatives **78** (Scheme 18c).<sup>[40]</sup> From a mechanistic standpoint, the addition to such chemical synthon proceeds as well to form  $\pi$ -allyl intermediate, in presence of chiral amine **31** and Pd(OAc)<sub>2</sub>. The best ligand for the reaction was found to be DPEPhos. Under the optimized conditions, 2-methyl-3-oxobutanoate could be added to the butadiene with 83% isolated yield and 93% enantioselectivity. The transformation could be successfully applied for the functionalization of many dicarbonyl derivatives, with isolated yields ranging from 66 to 90% and enantioselectivities from 84 to 95%.

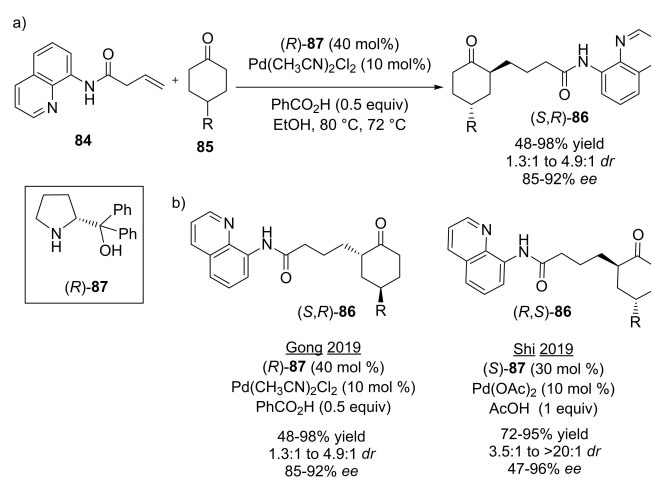
In 2019, Tian and co-workers developed a protocol for the preparations of structurally diverse  $\alpha,\alpha$ -disubstituted  $\beta$ -keto esters **81**, by means of cooperative palladium/enamine catalysis in presence of a chiral amino acid **83**. Its reaction with the ketoesters **80** leads to the formation of a chiral enamine which is able to react with the Pd- $\pi$ -allyl intermediate, formed in situ upon reaction between propargyl amine **81** and the metal. Also in this case, an internal directing group is able to stabilize the intermediate, leading to the formation of the new C–C bond in a stereoselective manner. Satisfying results were obtained in presence of electron-withdrawing (4-NO<sub>2</sub> and 4-CN) or electron-donating (4-Me) groups. The *E* and *Z* moieties undergo stereospecific nucleophilic attack from *Si* face and *Re* faces respectively, providing only two possible diastereoisomers (Scheme 19).<sup>[41]</sup>



**Scheme 19.** Stereoselective synthesis of  $\beta$ -keto esters.

Gong and co-workers introduced a method for the asymmetric alkylation of double bonds in presence of amides bearing an aminoquinoline as directing group.<sup>[42]</sup> The method involves the formation of a Pd<sup>II</sup> intermediate coordinating the allyl moiety (**84**), being stabilized by a directing group, present on the same molecule. The thus generated intermediate is able to react with a nucleophilic species. In this case, the authors proposed a series of ketones (**85**), able to react first with a chiral amine (*R*)-**87** to generate the corresponding chiral enamine. The umpolung could finally lead to a cooperative metal-enamine catalysis leading to the stereoselective formation of  $\alpha$ -branched ketone derivatives (*S,R*)-**86**. However, the process lacks of diastereoselectivity, being, the directing group, incapable to cooperate in the orientation of the nucleophilic attack (Scheme 20a). Synergistic palladium and enamine catalysis was explored further by Shi and co-workers to promote ketone addition to inactivated olefins.<sup>[43]</sup> The secondary amine-based organocatalyst (*S*)-**87** was identified as the optimal for the directed Pd-catalyzed alkene activation. Furthermore, asymmetric hydrocarbon functionalization of unactivated alkenes was also achieved with good to excellent yields (up to 96%) and stereoselectivities (up to 96% *ee*). This strategy represented an alternative approach to prepare  $\alpha$ -branched ketone derivatives under mild conditions (Scheme 20b).

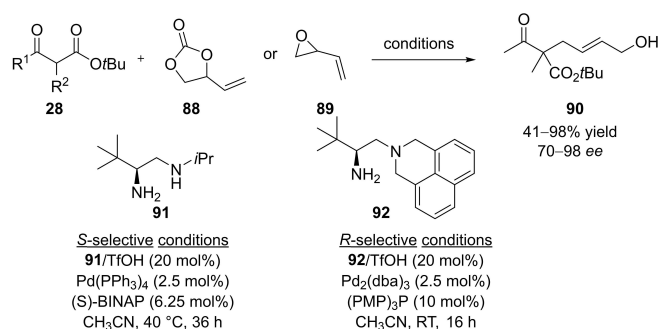
In 2020, Luo and co-workers reported the asymmetric addition of allyl carbonate **88** or allyl-epoxides **89** to 1,3-carbonyl derivatives **28**, exploiting the use of the chiral amine **91** or **92**, able to generate the competent nucleophilic enamine. This intermediate could react with vinyl ethylene carbonates or vinyl epoxydes, upon their coordination to palladium. The metal was revealed capable of coordinating the  $\pi$ -system of the double bond, providing an electrophilic species able to react with the enamine. The desired aldehydic products **90** could be obtained with high yields and enantioselectivities. Interestingly, for the preparation of the (*S*)-**90** a chiral phosphine ligand was required for the transformation, albeit for the synthesis of (*R*)-**90**, the racemic (PMP)<sub>3</sub>P has been employed. Such difference was attributed to a different stereocontrolling mode, operating



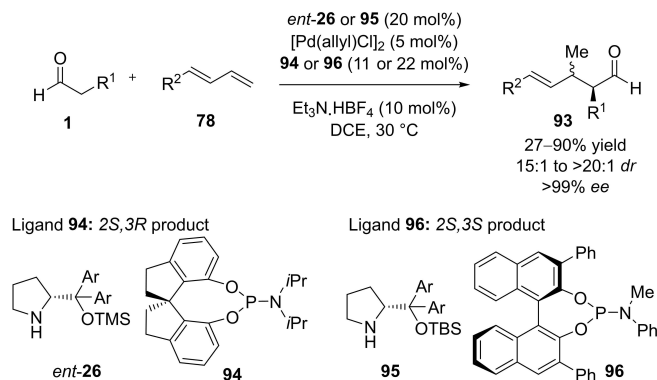
**Scheme 20.** Enantioselective synthesis of  $\alpha$ -branched ketone derivatives through directing group assistance.

differently within the two conditions. For the preparation of (*R*)-**90**, the aromatic chiral amine **92** was used, highlighting the existence of an aromatic  $\pi$ -coordinating event, able to drive selectively the attack of the nucleophile, thus, providing the corresponding product also in lower reaction time (Scheme 21).<sup>[44]</sup>

In 2021, Zi and co-workers proposed an enatio and diastereodivergent hydroalkylation process for the synthesis of enantiopure vinyl aldehydes. In their study, an alternative method was proposed for the synthesis of aldehydes with an enolizable proton, able to combine palladium-metal and enamine catalysis.<sup>[45]</sup> Efforts were provided to find the best chiral catalyst, able to coordinate efficiently the metal and lead to the formation of the corresponding metal-allyl electrophilic intermediate. The choice felt to electron deficient phosphoramidite-type ligand with a *spiro* backbone **94**, which offered the best enatio and diastereoselectivity when in presence of the chiral proline derivative *ent*-**26** or **95** (>99% *ee* and 20:1 *dr*). The optimized procedure could lead to the preparation of many different aldehydes from **1**, offering a complete stereodivergence by tuning the phosphine ligand and the amine respectively. Calculations could reveal the competence of the Brønsted acid Et<sub>3</sub>N·HBF<sub>4</sub> in the formation of Pd–H species from Pd<sup>0</sup>. Only at this point, the metal is able to coordinate the  $\pi$ -system of the allyl moiety generated from **78**, leading to the formation of the metal allyl intermediate (Scheme 22).



**Scheme 21.** Asymmetric addition of monoepoxides and allyl epoxides to 1,3 carbonyl derivatives.



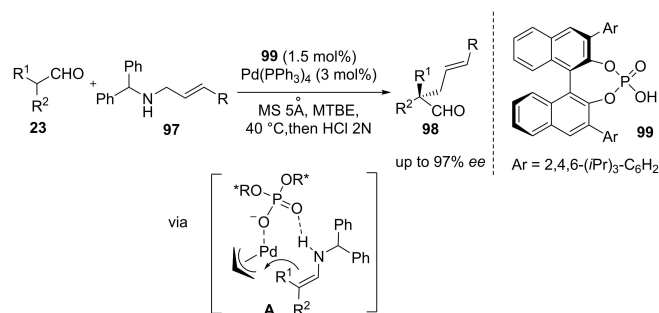
**Scheme 22.** Enatio- and diastereodivergent hydroalkylation for the synthesis of enantiopure vinyl aldehydes.

The group of List developed a pioneering procedure for the asymmetric  $\alpha$ -allylation of aldehydes **23** with allylic amines **97**, by the employ of a synergistic metal-chiral Brønsted acid catalysis. Excellent enantioselectivities could be obtained in presence of BINOL-based phosphoric acid **99**, able to serve as chiral counterion for the metal and mediating an outer sphere chirality transfer through ion pair interaction (ACDC).<sup>[46]</sup> Moreover, the Lewis basic site of **99** directs the achiral enamine attack through H-bonding (Scheme 23).<sup>[47]</sup>

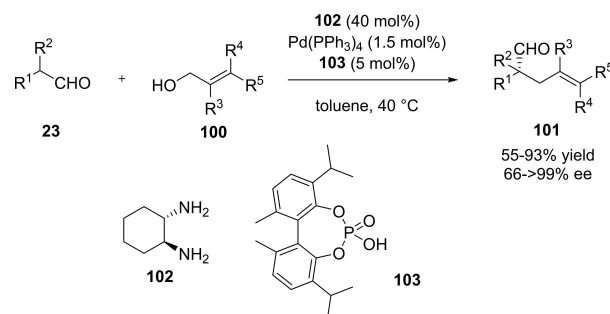
Inspired by these findings, Bica-Schröder and co-workers demonstrated alternatively that excellent enantioselectivities for the preparation of  $\gamma,\delta$ -unsaturated aldehydes **101** could be reached by introducing the use of a chiral diamine **102**, able to intercept the aldehyde **23** to form the corresponding chiral enamine, which traps the Pd–H-allyl intermediate formed in situ upon reaction with **100**. The employ of phosphoric acid **103** could serve as counterion for this cationic metal species (Scheme 24).<sup>[48]</sup>

### 3.4. Iminium ion-metal synergistic catalysis

Rios and co-workers developed a methodology for the asymmetric cyclopropanation of benzoxazole moieties **104** in presence of differently substituted unsaturated aldehydes **35**.<sup>[49]</sup> After reaction screening, the authors could find in 10 mol% of Pd(OAc)<sub>2</sub> and 20 mol% of Hayashi catalyst **18** the best conditions to isolate the product **105** with yields ranging from



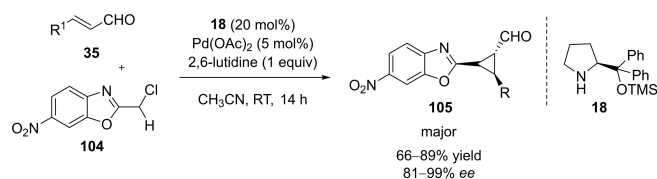
**Scheme 23.** Enantioselective  $\alpha$ -allylation of aldehydes by asymmetric counter-anion directed catalysis.



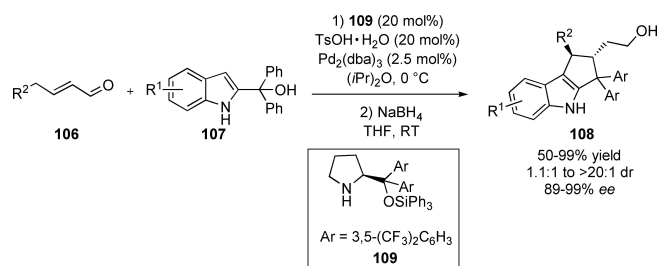
**Scheme 24.** Enantioselective  $\alpha$ -allylation of aldehydes with allylic alcohols with chiral diamines.

66 to 89% and 81 to 99% *ee* measured on the major reaction product (Scheme 25).

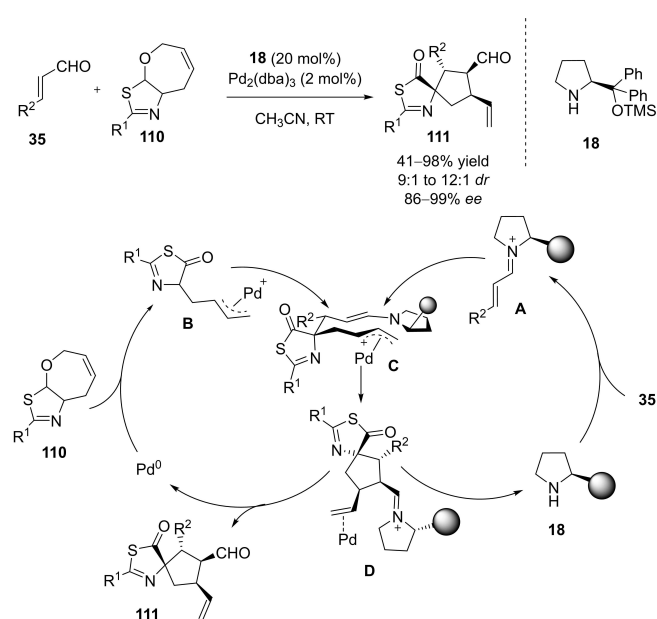
Cycloadditions represent another class of reactions able to outperform in asymmetric fashion via a synergistic metal iminium ion. Deng and co-workers established a procedure for an asymmetric [3 + 2] transformation involving 2-indolylmethanol derivatives **107** and  $\alpha,\beta$ -unsaturated aldehydes **106**, to provide the corresponding cyclopenta[*b*]indole derivatives **108**. Based on the proposed mechanism, the indolyl-methanol **107** undergoes dehydrative palladation first, to provide a cationic intermediate, which is subsequently attached by the chiral dienamine formed in situ, which is able to react intramolecularly



**Scheme 25.** Asymmetric cyclopropanation of bonzoxazoles.



**Scheme 26.** Asymmetric synthesis of cyclopenta[*b*]indole derivatives through [3 + 2] transformation.



**Scheme 27.** Cooperative procedure for the enantioselective synthesis of *spiro* derivatives.

in stereoselective manner. Further isomerization, followed by dehydration and reduction could provide the desired products with high diastereo- (up to 20:1) and enantioselectivities (up to 99%) (Scheme 26).

In 2021, Veselý and co-workers developed a cooperative procedure for the enantioselective synthesis of *spiro* derivatives starting from thiazole moieties, condensed with a 2,5-dihydrooxepine ring **110**.<sup>[50]</sup> Palladium(0) is involved in oxidative addition, forming the  $\pi$ -allyl **B** upon ring opening. The chiral iminium intermediate **A** formed in situ from condensation between aldehyde **35** and a chiral prolinol, **18**, is then trapped by the metallacycle **B**, bearing a nucleophilic carbon in  $\alpha$  to the carbonyl, to form the intermediate **C**, able to react intramolecularly with the electrophilic Pd– $\pi$ -allyl complex to provide the corresponding product of cyclization **D**, which undergoes hydrolysis to provide the desired product **111** (Scheme 27).

Despite the enormous progresses in the field, the  $\alpha$ -functionalization of carbonyl derivatives has been extensively investigated by combining amino catalysis with expensive rare-earth metals, thanks to their ability to form stable, electrophilic metallacycle intermediates. On the other hand, due to their higher accessibility in terms of costs and availability, earth-abundant transition metal catalysts represent a valuable alternative to pursue catalytic transformations. To date, the employ of such species for cooperative amino-metal catalysis still remains a challenge, being limited to only few reported examples.<sup>[51]</sup>

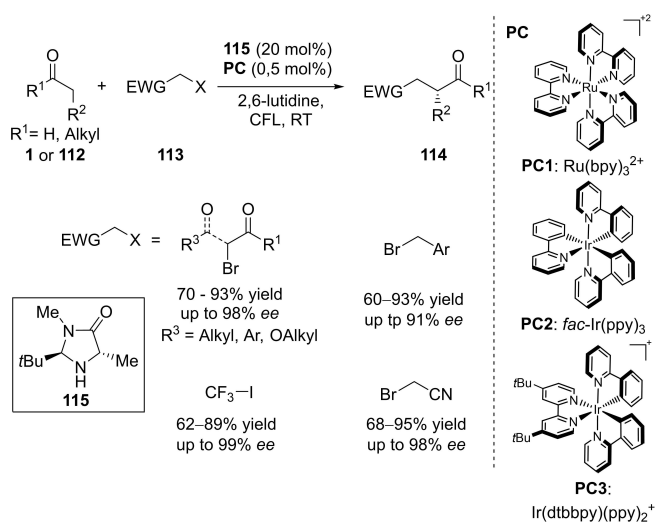
## 4. Amino-photoredox Synergistic Catalysis

### 4.1. General aspects

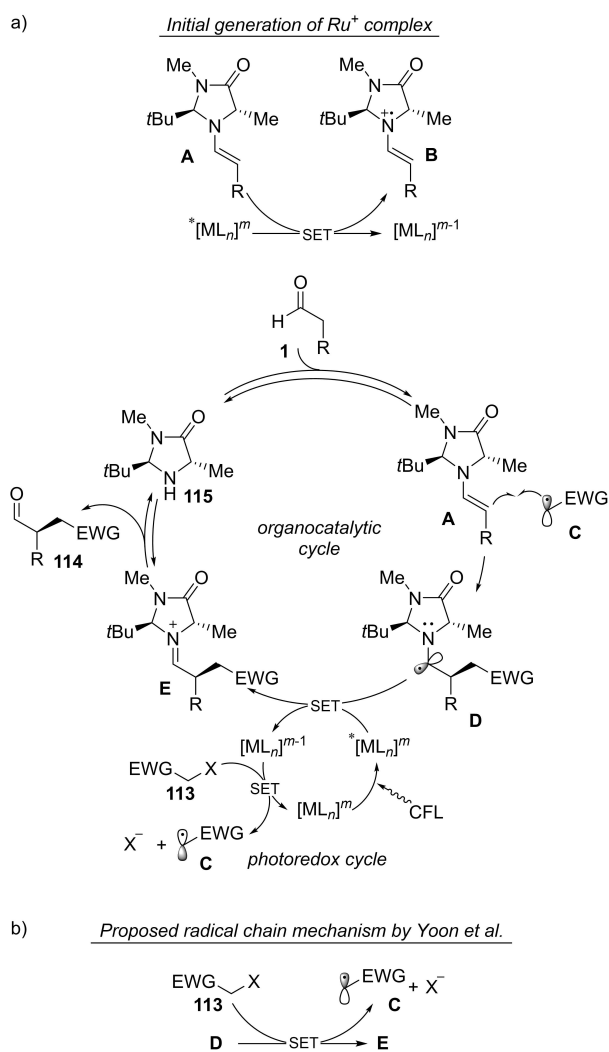
Amino-photoredox is undoubtedly one of the most exciting and fascinating research field in the last years. Combining together physical organic chemistry and aminocatalysis, it offers nowadays an incredible variety of synthetic tools, thanks to the above-mentioned ability of chiral amine to alter the energetic levels of the frontier orbitals of carbonyl compounds.<sup>[52,53]</sup> Given the significant discoveries in the field of photoredox-organocatalysis, the next section will be centred on the discussion of synergistic catalytic systems and the approaches based on one single catalyst able to activate both the substrates involved in the transformation. In the latter case, the aminocatalyst or its adducts (enamine or iminium ion) operates in the ground and in the photo-excited state simultaneously.

### 4.2. Early work

Building up on their experience on aminocatalysis and SOMO-catalysis<sup>[54]</sup> and on the ability of enamine to intercept electrophilic radicals,<sup>[55]</sup> MacMillan et al. realized the possibility of merging together a ground-state HOMO-raising activation of carbonyl compounds with a photoredox catalytic cycle that ensures the formation of an open shell species from alkyl halide in presence of light.<sup>[56]</sup> Employing chiral imidazolidinone **115**



**Scheme 28.** Synergistic enamine/photoredox catalysis for  $\alpha$ -functionalization of carbonyl compounds.



**Scheme 29.** a) General catalytic cycle for the synergistic amino/photoredox  $\alpha$ -alkylation of aldehydes with transition metal complexes as photocatalyst. b) Proposed radical chain mechanism.

and  $[\text{Ru}(\text{bpy})_3]^{2+}$  PC1 as photoredox catalyst (PC), it was possible to perform the  $\alpha$ -alkylation of aldehydes in high yield and excellent ee (Scheme 28).

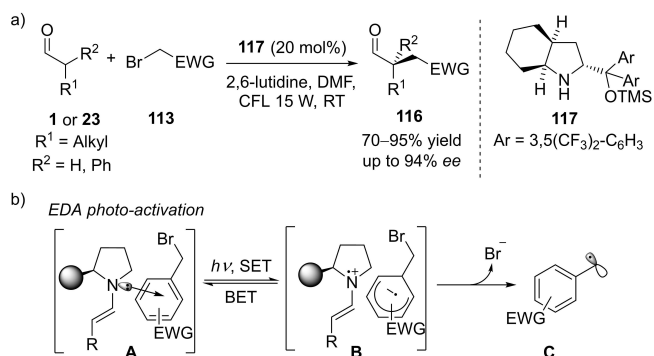
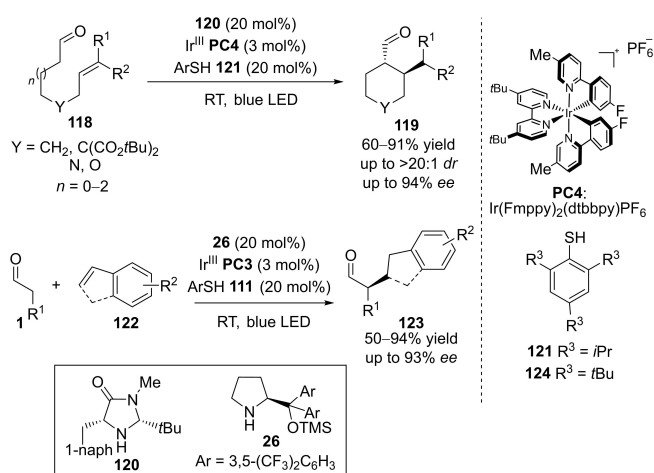
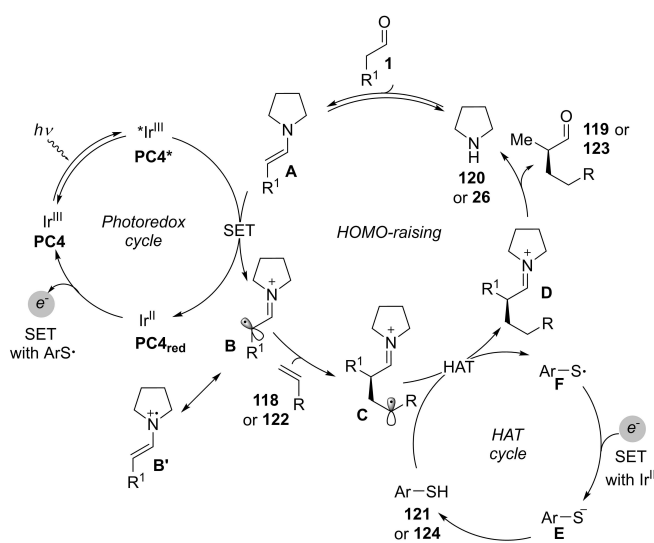
Based on the proposed mechanism,  $\alpha$ -bromo carbonyl substrates and carboxyl derivatives were converted by photoredox-induced single electron transfer (SET) to stabilized electrophilic radicals, and further intercepted by the enamine formed in situ.

In the reported seminal works (Scheme 29), the PC  $[\text{ML}_n]^m$  reaches the excited state  $^*[\text{ML}_n]^m$  upon photon absorption. This species could be further quenched by the enamine, acting as sacrificial electron donor. The resulting  $[\text{ML}_n]^{m-1}$   $[\text{Ru}(\text{bpy})_3]^{2+}$  /  $[\text{Ru}(\text{bpy})_3]^+$ , ( $E_{1/2}^{\text{red}} = -1.33$  V vs. SCE) is able to reduce the electron-poor alkyl halide 113 through SET, thus generating the corresponding electrophilic radical and restoring  $[\text{ML}_n]^m$ . C is intercepted by the enamine A forging the  $\alpha$ -amino radical D. On the mechanism proposed by MacMillan et al. in his seminal contribution the  $\alpha$ -amino radical D undergoes to a SET with  $^*[\text{ML}_n]^m$  ( $^*[\text{Ru}(\text{bpy})_3]^{2+}$ ) to close the photoredox catalytic cycle and affording the iminium ion E that hydrolyses to release the  $\alpha$ -functionalized carbonyl compound 114 and the imidazolidinone 115. In 2015, Yoon et al. reported on the  $\alpha$ -alkylation of aldehydes with bromo malonates employing  $[\text{Ru}(\text{bpy})_3]^{2+}$  measuring a quantum yield  $>1$  ( $\Phi = 18$ ) proposing that a radical chain propagation is in operation instead, a close photoredox catalytic cycle (Scheme 29b).<sup>[57]</sup>

The same strategy was applied also for the  $\alpha$ -functionalization of aldehydes with other electron-poor radical precursors such as aryl bromides,<sup>[58]</sup> bromo nitriles<sup>[59]</sup> and trifluoromethyl iodides.<sup>[60]</sup> On the latter,  $[\text{Ir}^{\text{III}}(\text{dtbbpy})(\text{ppy})]^{2+}$  was employed as PC (for  $^*\text{Ir}^{\text{III}}/\text{Ir}^{\text{II}}$   $E_{1/2}^{\text{red}} = -1.51$  V vs. SCE) able to reduce perfluoro alkyl iodides through SET ( $E_{1/2} = -1.33$  V vs. SCE). The benzylation with electron-poor benzyl bromide could be achieved in presence of *fac*- $\text{Ir}(\text{ppy})_3$  (for  $^*\text{Ir}^{\text{III}}/\text{Ir}^{\text{II}}$   $E_{1/2}^{\text{red}} = -1.73$  V vs. SCE; Scheme 28). More recently, this kind of strategy has been extended by employing organic photocatalyst,<sup>[61]</sup> inorganic heterogeneous photocatalysts,<sup>[62]</sup> and 3d-metal complexes<sup>[63]</sup> on the  $\alpha$ -alkylation of aldehydes and  $\alpha$ -branched ketones.<sup>[64]</sup>

In 2013, on the basis of a control experiment, Melchiorre et al. exploited the photoredox properties of organic electron donor acceptor (EDA) complexes<sup>[65]</sup> in the asymmetric  $\alpha$ -alkylation of aldehydes with electron-poor benzyl bromides and  $\alpha$ -bromo acetophenones affording the  $\alpha$ -alkylated aldehydes in excellent ee without the requirement of any other external photocatalyst (Scheme 30).<sup>[66]</sup>

The photo-active EDA complex A is formed at the ground state by the  $n \rightarrow \pi^*$  interaction between the enamine and 113 (Scheme 30b). Irradiation of A with a 15 W CFL induces an electron transfer arising to the radical ions pair B. It is important to notice that this process is reversible and that a back electron transfer (BET) could restore the starting materials without the irreversible C–X bond cleavage. The electrophilic radical C can be then intercepted in an enantioselective fashion by the chiral enamine on radical-chain-type reaction ( $\Phi = 25$ ).<sup>[67]</sup>

Scheme 30.  $\alpha$ -Alkylation of aldehydes driven by EDA complexes.Scheme 31.  $\alpha$ -Alkylation of aldehydes with simple olefins.Scheme 32.  $\alpha$ -Alkylation of aldehydes with styrene-driven enamine/photoredox/HAT synergistic catalysis.

## 4.3. Enamine-photoredox synergistic catalysis

The scope of enamine-photoredox catalysis was extended to  $3\pi e^-$  carbonyl systems by MacMillan et al. in 2017, exploiting the synergistic combination of three catalytic cycles: enamine, photoredox and hydrogen-atom transfer (HAT).<sup>[53]</sup> Early studies were made on the developed of inter- and intramolecular  $\alpha$ -alkylation of aldehydes with simple olefins in presence of blue led<sup>[68]</sup> employing either catalyst 26 or imidazolidinone 120 in presence of Ir<sup>III</sup> photocatalyst PC4 and sterically demanding thiophenol 121 or 124 the alkylated products 119 and 123 were obtained in high yield and ee with a broad scope (Scheme 31).

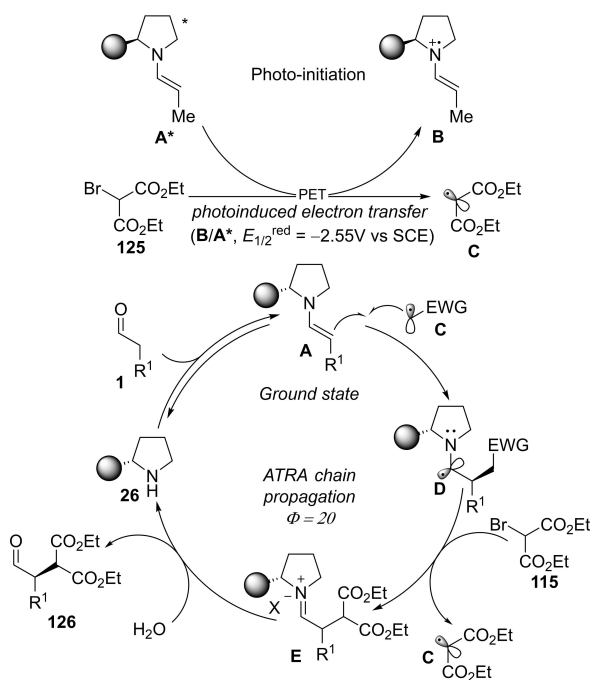
The reaction design involves two SET and one HAT across a tricatalytic overall redox neutral process with remarkable selectivity (Scheme 32).

Ir<sup>III</sup> PC4 undergoes to photo-excitation forming the oxidant \*Ir<sup>III</sup> PC4\* (for \*Ir<sup>III</sup> PC4\*/Ir<sup>III</sup> PC4<sub>red</sub>,  $E_{1/2}^{red} = +0.77$  V vs. SCE), that synergistically with the HOMO-raising activated aldehyde A is forming the key  $3\pi e^-$  iminyl radical cation B (in resonance with B'). This open-shell species intercepts the olefin 122 forming a new stereodefined C–C bond in the nucleophilic radical C. The thiophenol 121 or 124 (HAT catalytic cycle) quenches C generating the iminium ion D, that undergoes to hydrolysis affording the  $\alpha$ -alkylated product 119 or 123 and the thiol radical F. Finally, a SET between Ir<sup>II</sup> PC4<sub>red</sub> (for Ir<sup>III</sup> PC4/Ir<sup>II</sup> PC4<sub>red</sub>,  $E_{1/2}^{red} = +1.55$  V vs. SCE) and F (for PhS<sup>•</sup>/PhS<sup>-</sup>,  $E_{1/2}^{red} = -0.02$  V) close both the HAT and the photoredox cycle upon protonation of the aryl thiolate E.

Through an intensive study,<sup>[69]</sup> Melchiorre et al. envisaged the possibility of employing an electron-rich enamine intermediate not only for the  $\alpha$ -activation of carbonyl compounds on the ground state but also, upon photo-excitation, as photocatalytic single electron reductant.

This discovery raised up by the observation that bromo malonates were suitable substrates for the  $\alpha$ -alkylation of aldehydes without the use of any photocatalyst or EDA complex formation. With this concept in hand, the authors performed the  $\alpha$ -alkylation of aldehydes with bromomalonate<sup>[70]</sup> and (phenylsulfonyl)alkyl iodides<sup>[71]</sup> using only Jørgensen/Hayashi catalyst 26 under 23 W CFL irradiation obtaining the corresponding products on high yield and ee.

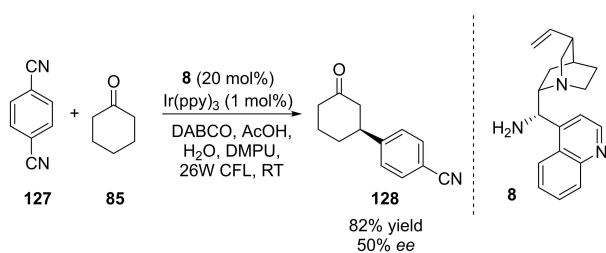
In Scheme 33, the mechanism of  $\alpha$ -alkylation with bromomalonates is reported. The reaction is initiated by the photo-excitation of enamine A generated in situ resulting in A\* ( $E_{1/2}^{red} = -2.55$  V vs. SCE) promoting its selective photoinduced electron transfer (PET) with 125 ( $E_{1/2}^{red} = -0.49$  V vs. SCE). The irreversible reductive fragmentation of 125<sup>•-</sup> (not shown) forms the electrophilic radical C that reacts enantioselectively with the ground state enamine A. The chain propagation event ( $\Phi = 20$ ) is likely different from the one in Scheme 29b. Indeed, D is not suitable for reducing the bromomalonate 125, although it can abstract a bromine radical from 125 collapsing into the iminium ion E and generating the electron-poor radical C. This strategy is governed by the dichotomous behavior of the enamine A able to promote a photoinduced single electron reduction of the radical precursor and, on its ground state, to ensure the



**Scheme 33.**  $\alpha$ -Alkylation of aldehydes with bromomalonate driven by synergistic ground-/photoexcited-state enamine catalysis.

stereoselection of the reaction in ATRA process. The  $\alpha$ -methylsulphonation of aldehydes proceeds in analogously to the mechanism reported in Scheme 33.

One of the challenges of asymmetric photoredox enamine catalysis, despite the chemistry is already on place, is the development of enantioselective functionalization of saturated carbonyl compounds. MacMillan et al. realized that a  $3\pi e^-$  enaminy radical cation (Scheme 32 see **B'**) possesses an increased  $\beta$ -proton acidity with respect to the electron-rich ground state enamine. As consequence, they envisaged the possibility of expanding the  $3\pi e^-$  reactivity through a Brønsted base deprotonation accessing a  $5\pi e^-$  catalytic platform.<sup>[72]</sup> Submitting a carbonyl compound **85** to an enamine/Ir<sup>III</sup> synergistic catalysis in presence of stabilized radical precursor such as 1,4-dicyanobenzene **127** the  $\beta$ -arylated product was obtained in high yield. Interestingly, employing *Cinchona* derived primary amine **8** as organocatalyst the reaction shown a promising stereoselectivity (Scheme 34).<sup>[72c]</sup>



**Scheme 34.**  $\beta$ -Arylation of saturated carbonyl compounds through enamine/Ir<sup>III</sup> synergistic catalysis.

In 2020,  $5\pi e^-$  amino-photoredox was applied by MacMillan et al. to the stereo ablation of  $\beta$ -substituted cyclic ketones *rac*-**129**. Moreover, coupling the reversible  $\beta$ -enaminy radical **C** formation with ketoreductase catalyzed kinetic resolution, the authors designed the DKR of racemic  $\beta$ -substituted cyclic ketones *rac*-**129** affording  $\gamma$ -substituted alcohols **130** in outstanding *ee*.<sup>[73]</sup> Notably, by tuning the catalyst system, it was possible to access to all four the stereoisomers of the product as a single enantiomer. The synergistic enamine/photoredox stereoablative process enables the fast equilibration between the two enantiomers of the  $\beta$ -branched ketone *rac*-**129**, while the biocatalytic cycle selectively reduces one enantiomer of it (in the case shown below the (*R*)-**129**; Scheme 35). Aminocatalyst **131** activates *rac*-**129** through HOMO-raising favoring the SET oxidation (for (*S*)-**A**  $\rightarrow$  (*S*)-**A**<sup>•+</sup> half-peak potential  $E_p = +0.33$  V vs. SCE in MeCN)<sup>[74]</sup> by means of the photoexcited \*Ir<sup>III</sup> PC5\* (for \*Ir<sup>III</sup> PC5\*/Ir<sup>II</sup> PC5<sub>red</sub>  $E_{1/2}^{red} = +1.21$  V vs. SCE in MeCN) resulting in Ir<sup>II</sup> PC5<sub>red</sub> and the  $3\pi e^-$  enaminy radical cation (*S*)-**A**.

This intermediate possesses a pronounced  $\beta$ -acidity and undergoing to an allylic deprotonation forms the stereoablated key  $5\pi e^-$  specie **C**. *p*-methoxy thiol **132** transfers an H<sup>•</sup> unselectively to **C** (HAT cycle) and later enamine hydrolysis released the cyclic ketone enantiomers (*S*)-**A** and (*S*)-**A** together with the aminocatalyst **131**. The photoredox and the HAT cycles converge by a SET between **E** and Ir<sup>II</sup> PC5<sub>red</sub> restoring the ground state Ir<sup>III</sup> photocatalyst PC5 and **D** (for Ir<sup>III</sup> PC5/Ir<sup>II</sup> PC5<sub>red</sub>  $E_{1/2}^{red} = -1.37$  V vs. SCE in MeCN), (for ArS<sup>•</sup> E/ArS<sup>-</sup> **D**  $E_{1/2}^{red} = -0.06$  V vs. SCE in MeCN). Finally, **D** undergoes to a protonation regenerating **132** HAT catalyst. These three catalytic cycles work in concert for ensuring the racemization of the kinetic unfavorable (*S*)-**129** enantiomer with respect to the biocatalytic carbonyl reduction (Scheme 35).

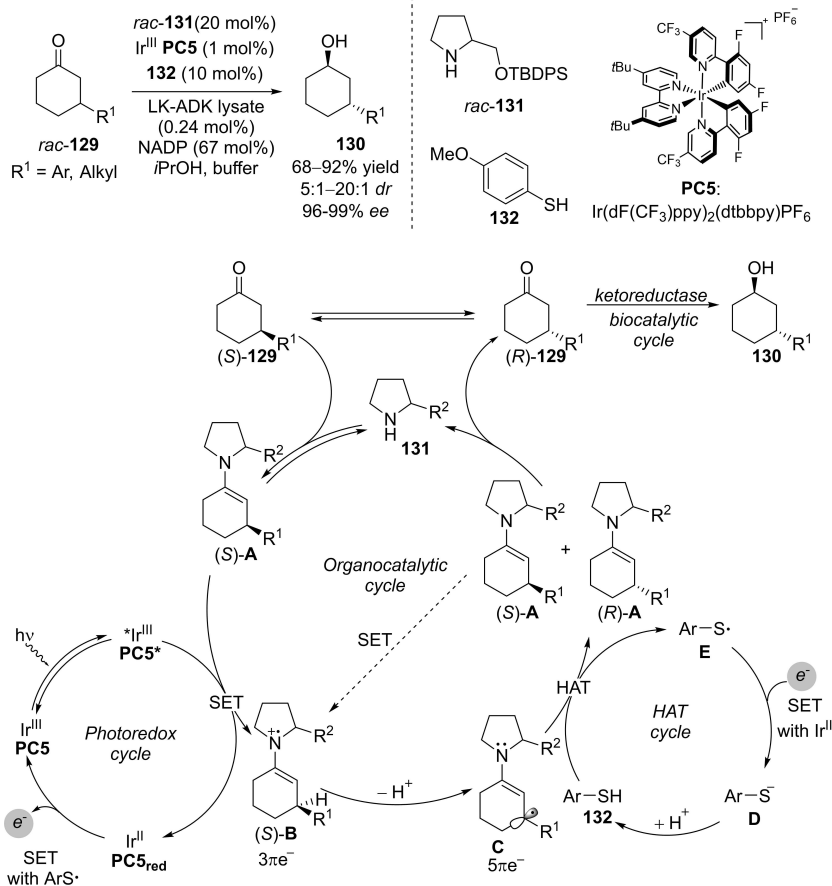
In 2022, inspired by the contributions of Bach<sup>[75]</sup> and Knowles<sup>[76]</sup> reporting the photocatalytic deracemization of allenes and ureas through the synergistic use of organocatalysis and light, Luo et al. developed the HOMO-raising/photoredox synergistic deracemization of  $\alpha$ -branched aldehydes *rac*-**23** (Scheme 36).<sup>[77]</sup>

The strategy relies on the photo-isomerization of the key enamines intermediates **A** and **B** as well as on their different stability (**A** is more stable than **B**). The photoisomerization is proposed to occur by means of energy transfer between the triplet state of **PC2** and the enamines. In this elegant process, the formation of the energetically favored (*E*)-enamine **A** through condensation of **133** with (*S*)-**23** ensures the depletion of the enantiomer while protonation of the (*Z*)-enamine arises to an accumulation of (*R*)-**23** (Scheme 36b).

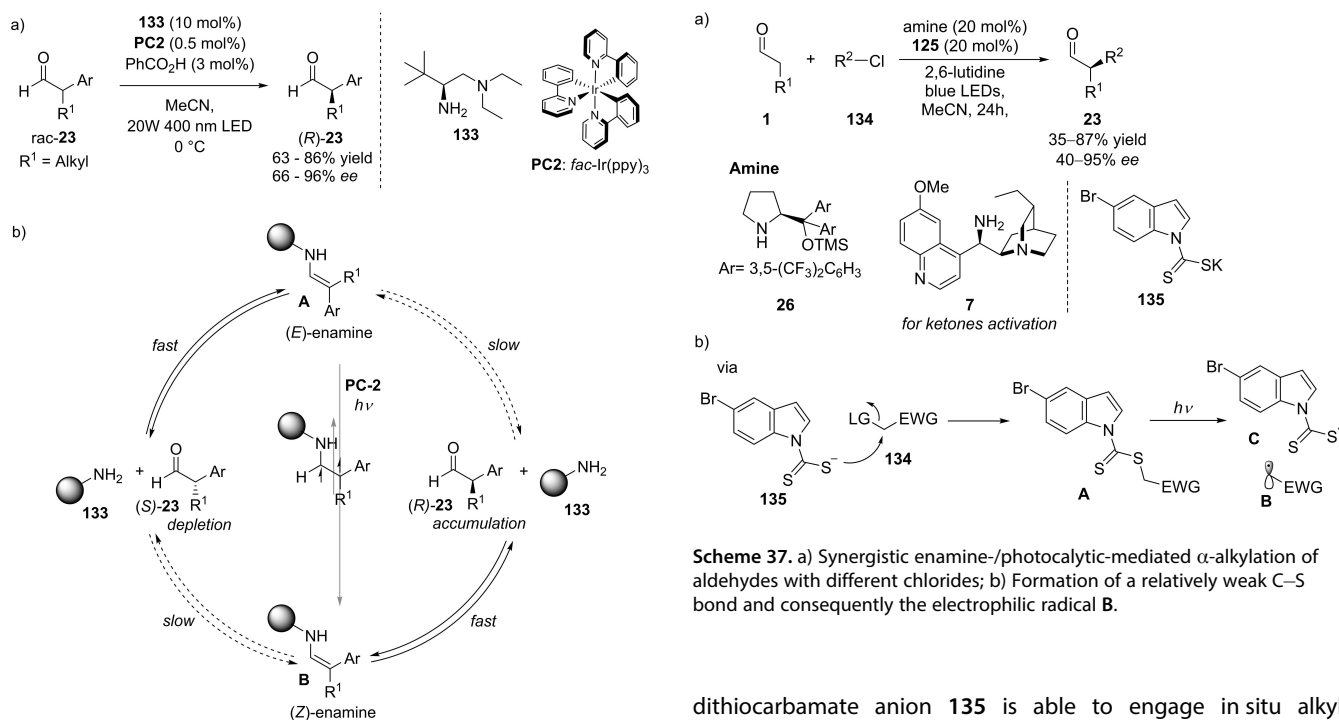
Nowadays, amino-photoredox catalysis is, despite some debates, a well-established strategy that relies on SETs across different catalytic cycles of the reaction. Classical radical chemistry is on the other hand founded on the homolytic cleavage of weak bonds for the generation of the reactive open-shell species.

Melchiorre et al., employing Jørgensen/Hayashi catalyst **26** in presence of a dithiocarbamate anion **135** as nucleophilic photocatalyst performed the  $\alpha$ -alkylation of aldehydes with various chlorides as starting materials (Scheme 37a).<sup>[78]</sup> The

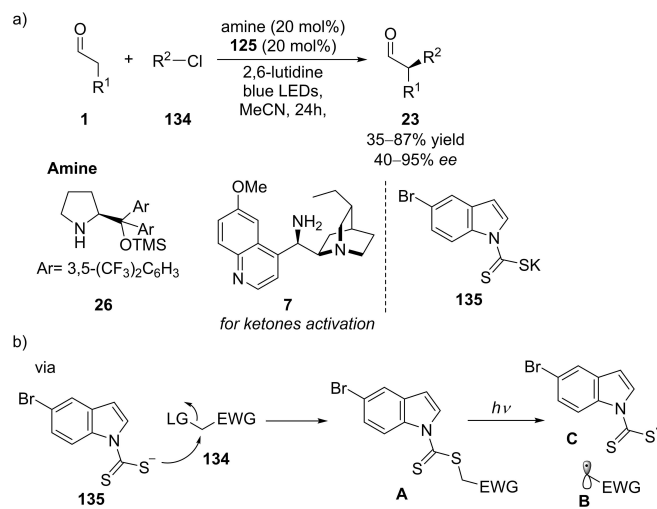




**Scheme 35.** Mechanistic insight into the synergistic enamine/photoredox/biocatalysis of the DKR of  $\beta$ -substituted cyclic ketones.



**Scheme 36.** Deracemization of  $\alpha$ -branched aldehydes by synergistic use of aminocatalysis and light.



**Scheme 37.** a) Synergistic enamine/photocatalytic-mediated  $\alpha$ -alkylation of aldehydes with different chlorides; b) Formation of a relatively weak C–S bond and consequently the electrophilic radical B.

dithiocarbamate anion **135** is able to engage in situ alkyl chlorides **133** in a  $S_N2$  process, forming a relatively weak C–S bond BDE (for benzyl dimethylthiocarbamate BDE = 31.3 kcal mol<sup>-1</sup>). It is noteworthy that the reducing potential of

alkyl chlorides are generally out of reach of well-established photoredox catalysts (for  $\text{Bn-Cl/Bn}^{\cdot-}\text{Cl}^-$   $E_{1/2}^{\text{red}} = -2.13$  V vs. SCE). The indole moiety acts as an antenna favoring the photon-induced homolytic cleavage, generating the electrophilic radical **B** and **C** (Scheme 37b).

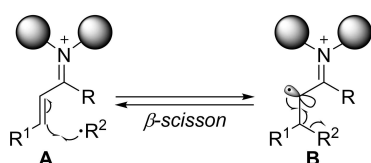
The ground state enamine intercepts the open-shell species **B** in analogy with Scheme 29.

Dithiocarbamate anion **135** was employed also by the same authors to the photocatalytic Giese-type reaction under mild conditions, allowing the functionalization of a vast array of Michael acceptors<sup>[79]</sup> as well as for the  $\alpha$ -alkylation of ketones, relying on the less sterically demanding primary amine **7**.<sup>[80]</sup>

#### 4.4. Iminium ion-photoredox synergistic catalysis

LUMO-lowering activation in photoredox aminocatalysis<sup>[81]</sup> especially the addition of nucleophilic radical species to the electron-poor iminium ion **A**, was hampered by the reversible nature of the  $\alpha$ -iminyl radical cation intermediate **B** (Figure 3).

##### a) Challenge on radical addition to iminium ion intermediates



##### b) Melchiorre et al. strategy

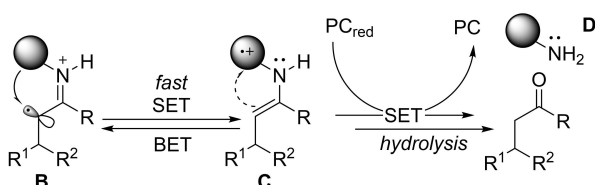
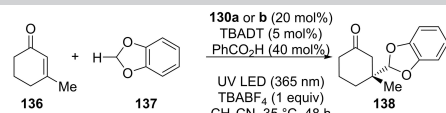


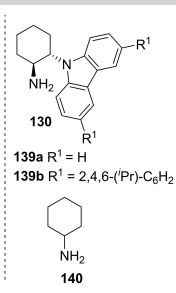
**Figure 3.** a) Challenges in radical addition to iminium ion intermediates. b) Aminocatalyzed reduction through intramolecular SET of the  $\alpha$ -iminyl radical cation followed by the formation of the photoactive catalyst **D**.

**Table 2.** Selected examples in catalyst design for the 1,4-addition of radical to  $\beta$ -enones by synergistic amino-photoredox catalysis.



Entry	Catalyst	Yield [%]	ee%
1	<b>139a</b>	33	82
2	<b>139b</b>	46	93
3 <sup>[a]</sup>	<b>140</b>	<5	---
4	none	<5	---

[a]: 20 mol% of carbazole



**130**  $\text{R}^1 = \text{H}$   
**139a**  $\text{R}^1 = \text{H}$   
**139b**  $\text{R}^1 = 2,4,6\text{-}i\text{Pr-C}_6\text{H}_2$   
**140**

Moreover, this intermediate is reported to undergo fast stereo-ablation in presence of a Brønsted base. Melchiorre et al. envisaged that the use of an aminocatalyst, able to quickly reduce through intramolecular SET the  $\alpha$ -iminyl radical cation **B**, could drive it to the enamine **C**. In order to preclude BET, a primary amine was chosen, since secondary enamine stays in equilibrium with the predominant electron-poor imine form (not shown). In the designing of the photocatalyst **D**, chiral 1,2-cyclohexan diamine core was adorned with redox active carbazole moieties and tested on the conjugate addition of benzodioxole **137** derived radical to  $\beta$ -methyl cyclohexanone **136**, in presence of tetrabutylammonium decatungstate (TBADT, 5 mol%) as photocatalyst (Table 2).<sup>[83]</sup>

Simple carbazole substituted aminocatalyst **139a** ( $E_p^{\text{ox}} = +1.15$  V,  $E_p^{\text{red}} = -1.32$  V) catalyzed the reaction with promising yield and enantiomeric excess. Relying on the fact that 3,6-substituted carbazole can further stabilize the radical cation and introducing a privileged electron-rich steric moiety (2,4,6-*i*Pr-C<sub>6</sub>H<sub>2</sub>), the authors synthesized the aminocatalyst **139b** ( $E_p^{\text{ox}} = +1.10$  V,  $E_p^{\text{red}} = -1.38$  V) that forges the product **138** in good yield and up to 93% ee. Interestingly, employing **140** and 20 mol% of *N*-cyclohexyl-3,6-di-*tert*-carbazole the reaction does not occur, pointing out the key role of a proximity-induced single electron transfer (SET). This amino-photoredox synergistic strategy was applied for the stereoselective formation of  $\beta,\beta$ -disubstituted cycloketones with benzodioxole or anilines as radical precursor in presence of TBADT or Ir<sup>III</sup>-PC5 as photocatalyst (Scheme 38).

The excited photocatalyst (**PC\***) is responsible for the initial formation of the nucleophilic radical **D** that intercepts the iminium ion **A**, arising to the key  $\alpha$ -iminyl radical **B**. This intermediate undergoes to a proximity-induced SET forming the enamine **C**. Finally, SET between **PC<sub>red</sub>** and **C** followed by hydrolysis restore the photocatalyst **PC** and **139b** affording the desired products in high yields and ee.

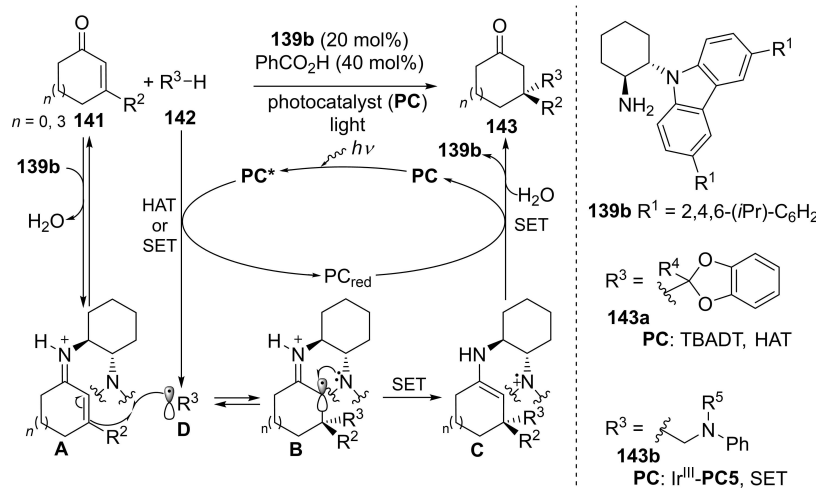
Building up on these results and on their knowledge of amino-photoredox catalysis by EDA complexes, Melchiorre et al. observed through X-ray spectroscopy the formation of an intramolecular EDA complex as feature of the iminium ion **A**.

Employing the aminocatalyst **139c** (Scheme 39), the authors were able to perform the functionalization of ketones with various silylated radical precursors in good yields and enantiomeric excess.<sup>[84]</sup> In this reaction, the iminium ion/EDA complex **A** (carbazole moiety:  $\pi$ -donor / iminium ion:  $\pi^*$ -acceptor) is converted into **B** upon light absorption and intramolecular SET.

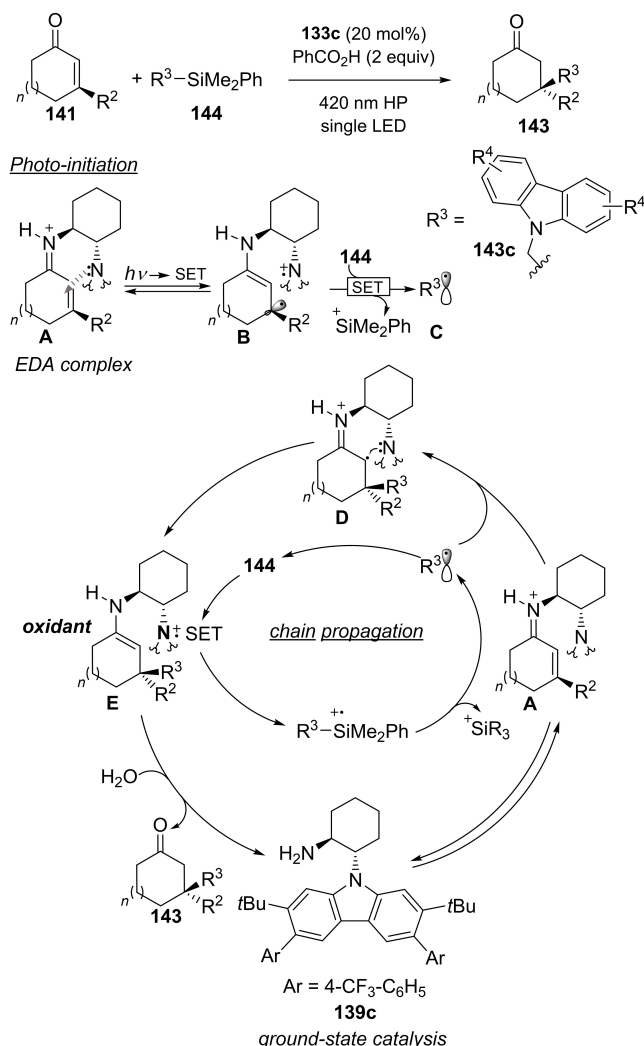
The persistent radical cation **B** can oxidize the radical **144** driving it to the radical **C** formation through mesolysis. The ground state iminium ion **A** can intercept **C** enantioselectively.

After that, the carbazole moiety precludes the  $\beta$ -scission through a proximity-induced SET from the carbazole to the  $\alpha$ -iminyl radical **D**. The carbazole radical cation present in this intermediate, continues the radical chain through a SET with another molecule of **144**. Hydrolysis of the enamine that arises after the process results into the product **143** and favours the regeneration of catalyst **139c**. Promising results were obtained also employing other radical precursors.

The opposite but yet similar nature of HOMO-raising and LUMO-lowering activation<sup>[2k]</sup> inspired Melchiorre et al. to inves-



**Scheme 38.** Amino-photoredox synergistic methodology for the stereoselective formation of  $\beta,\beta$ -disubstituted cycloketones with benzodioxole or anilines.



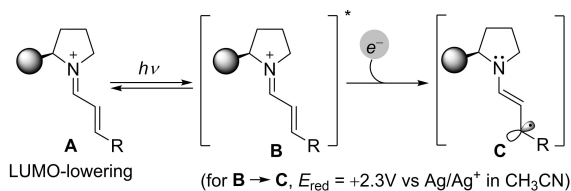
**Scheme 39.** Functionalization of ketones with various silylated radical precursors through intramolecular EDA complex formation.

investigate the photoredox behavior of iminium ion.<sup>[65]</sup> Irradiating the ground state iminium ion, the authors unlocked its excited state reactivity. In presence of 420 nm light source, this intermediate becomes a strong single electron oxidant (Scheme 40).

Testing this new concept in the reaction between cinnamaldehyde **40** and benzyl trimethylsilane **138**, it was shown in Stern-Volmer studies that **B** undergoes to quenching in presence of **138**. As for other photo-redox protocols, this benzyl radical precursor undergoes to SET and desilylation, hampering the BET. One of the challenges of this photoredox reactivity arises from the high oxidation potential of **B**, that drives the free electron-rich amino-catalyst to decomposition. An elegant design of the steric and electronic properties of the catalyst was crucial for accessing  $\beta$ -benzylated aldehydes **139** in outstanding yield and *ee* (Table 3).

The catalyst screening showed how privileged chiral amines are unsuitable for this transformation. MacMillan imidazolidinone **4** provides the desired product in high yield but low enantiocontrol (entry 1). On the other hand, OTDS protected Jørgensen/Hayashi catalyst gives promising *ee* but no turnover (entry 2). This was ascribed to the low oxidation potential of **147**, and consequently to its decomposition due to **B** (oxidant). In this scenario the rational design of gem-difluorinated amino-catalyst **148** ( $E^{\text{ox}}$  (**148**<sup>•+</sup>/**148**) = +2.20 V vs. Ag/Ag<sup>+</sup> in CH<sub>3</sub>CN) was fundamental for achieving high yields and good enantiomeric excess (entry 3). Finally, tailoring the aryl moieties of the new Jørgensen/Hayashi-type catalyst, installing more stereo-demanding groups, the authors synthesized **149**, able to catalyze the reaction, providing high yields and excellent *ee*.

The scope of this transformation is not only limited to  $\beta$ -benzylation of aldehydes, but also to a wide array of electron-rich radical moieties, employed as silylated precursors. Analogously to the HOMO-raising photoredox counterpart, the ground state LUMO-lowering activation and the photo excited iminium-ion, acts synergistically in the catalytic cycle (Scheme 41).



**Scheme 40.** Melchiorre et al.'s investigation of the photoredox behavior of the iminium ion.

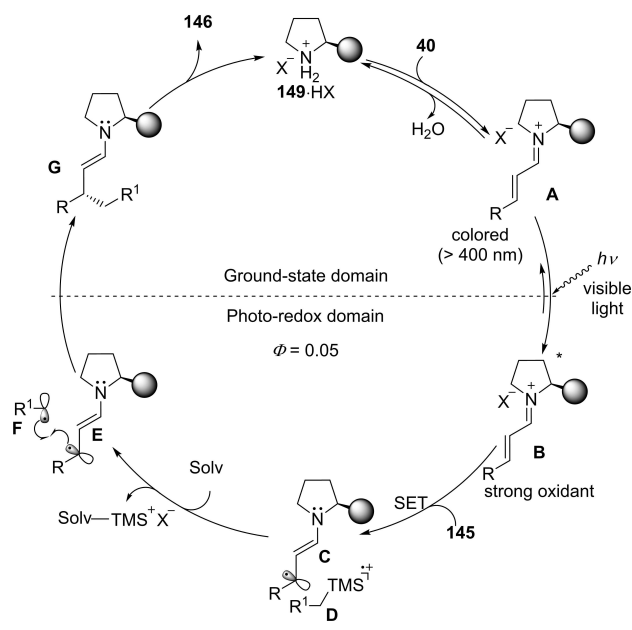
**Table 3.**  $\beta$ -Benzylation of aldehydes through synergistic ground-/photo-excited-state iminium ion catalysis.

Amine	Yield [%]	ee [%]
1	79	30
2	28	76
3	83	85
4	87	88

On the proposed mechanism, the catalytic salt **149**-TFA lowers the LUMO energy of the  $\beta$ -enal **40** through the formation of an iminium ion intermediate **A** (ground state domain). Upon light absorption (photo-redox domain), the iminium ion becomes a strong oxidant, thus triggering a SET with the radical precursors **145**. Subsequently, mesolysis drives it to the open-shell species **F** that undergoes stereoselective coupling with the  $5\pi e^-$  enaminy radical **E** ( $\Phi = 0.05$ ). Back on the ground state domain, hydrolysis of the enamine **G** regenerates the amino-catalyst **149** affording the final product **146**. This strategy has also been applied to different stereoselective  $\beta$ -functionalizations.<sup>[86]</sup>

The strong oxidation power of photo-excited iminium ion, allows to this intermediate to remove an electron directly from toluene ( $E^{\text{ox}} = +2.26 \text{ V vs. SCE}$ ). The absence of any redox-auxiliary group (i.e.,  $R^3\text{Si}$ ) results in a fast BET process, leading to the regeneration of the starting materials.

In this scenario, Melchiorre et al. envisaged that a deprotonation of the transient benzyl radical **C** ( $pK_a = -13$  in  $\text{CH}_3\text{CN}$ )

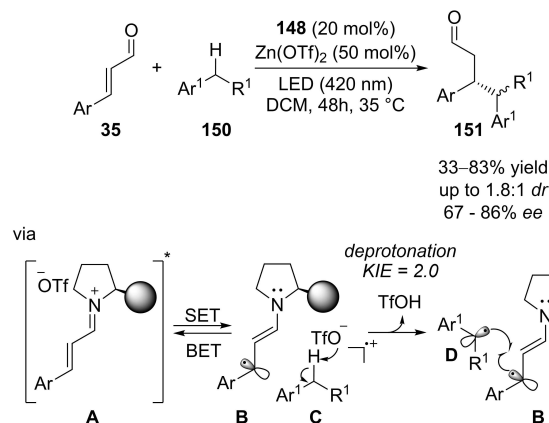


**Scheme 41.** Mechanistic insight into the  $\beta$ -functionalization of aldehydes through synergistic ground-state/photoexcited-state iminium ion catalysis.

would form the more stable benzyl radical **D** able to couple with the  $5\pi e^-$   $\beta$ -enaminy radical **B** (Scheme 42).<sup>[87]</sup>

In addition to the optimization of the photoredox system, the key point of the transformation is the deprotonation step, as also underlined by the  $k_D/k_H$  kinetic isotope effect ( $\text{KIE} = 2.0$ ). The counter-anion of the iminium ion is responsible of the synergistic abstraction of the acidic proton from **C**. In this regard, the choice of  $\text{Zn}(\text{OTf})_2$  resulted critical. It was proposed that the Lewis acidic  $\text{Zn}^{2+}$  enhances the iminium ion formation rate, while the triflate secures the deprotonation. The employment of the photo-excited iminium ion as SET oxidant is restricted to aromatic  $\beta$ -enals ( $\lambda_{\text{abs}} < 430 \text{ nm}$ ), since in presence of aliphatic substrates, the absorption is in the near UV.

Noteworthy, the introduction of aminocatalyst **148** resulted pivotal also for the development of a general protocol for the  $\beta$ -alkylation of aliphatic and aromatic  $\alpha,\beta$ -unsaturated alde-



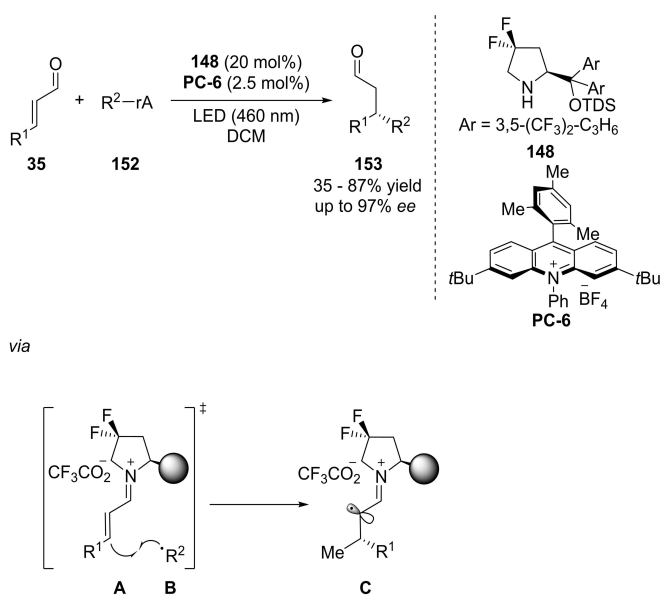
**Scheme 42.** Enantioselective  $\beta$ -benzylation of enals with toluene derivatives.

hydrides **35**.<sup>[88]</sup> The scope of this reaction includes several radical precursors **152** decorated with a suitable redox-auxiliary (rA; Scheme 43).

In this synergistic catalytic system, the photoredox cycle is ensured by the highly oxidant acridium tetrafluoroborate **PC-6** ( $E^*(\text{PC-6}^*/\text{PC-6}^{\bullet-}) = +2.08 \text{ V vs. SCE in CH}_3\text{CN}$ ) capable of being selectively photoexcited ( $\lambda_{\text{max}} = 460 \text{ nm}$ ). Upon irradiation **PC-6** triggers the radical formation from **152**. This radical **B** intercepts the iminium ion **A** converting it to **C**. A SET between the  $\alpha$ -iminyl radical cation **C** and the reduced acridinium **PC-6<sup>•-</sup>** regenerates the photocatalyst closing the amino/photoredox cycle ( $\Phi = 0.02$ ). Notably the high redox potential of the aminocatalyst **148** prevents its decomposition.

The advent of synergistic amino/photoredox catalysis, sets up the stage for challenging and sometimes unreported transformations in the whole field of asymmetric catalysis. Moreover, likewise in the beginning of 2000s, HOMO-raising and LUMO-lowering activation of carbonyl compounds are leading the development of organocatalysis also in this paradigm. It is worth of mention, that the potentialities of aminocatalysis are far to be exhausted. As plausible target of investigation, new catalysts will be selected to extend the strategy to remote functionalization and to the control of prochiral radicals.

In this section are reported selected pioneering reports although the number of actors in this field is expanding tremendously. In our opinion, one of the main challenges of amino/photoredox synergistic catalysis is the use of low-power visible light for all the transformations, ideally sunlight.



**Scheme 43.**  $\beta$ -Alkylation of aliphatic and aromatic  $\alpha,\beta$ -unsaturated aldehydes through synergistic iminium ion/photoredox catalysis.

## 5. Synergistic Use of Aminocatalysis and Electrochemistry

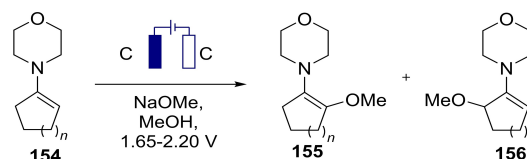
### 5.1. General aspects

In recent years, electrochemistry applied to organic chemistry and synthesis gained a pivotal role in the arena of chemical transformations, finding practical applications in both reductive and oxidative transformations.<sup>[89]</sup> With the acquired possibility to deliver precise amounts of electrons into the reaction media, a more significant number of chemical transformations could be finally achieved, avoiding the use of polluting reagents such as stoichiometric base metals or chemical oxidants, ensuring a milder reaction environment. As a consequence, an extensive array of reactions could finally be performed within milder and greener conditions. HOMO-raising activation of carbonyl compounds through aminocatalysts offers the unique possibility of inducing the formation and controlling the stereo-induction of reactive radical intermediates also in this field.

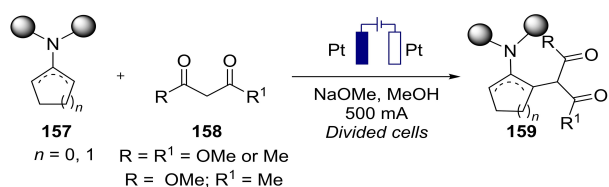
### 5.2. Early work

Early work on electrochemistry applied to enamine catalysis was reported by Shono et al. in 1978. The authors proposed the anodic oxidation of enamines **154** in presence of methanol, observing the formation of two products of methoxylation **155** and **156** (Scheme 44).<sup>[90]</sup>

This procedure reports on the oxidation of vinylic and allylic position of the enamine **154** upon treatment with sodium methoxide as supporting electrolyte and carbon rods as anode-cathode couple. The system could develop 3 F/mol electrons, working at current values ranging from 1.65 to 2.20 V (vs. SCE). The final products **155** and **156** could be isolated albeit a difficult separation of the isomers was encountered. One year later,<sup>[91]</sup> Chiba et al. reported the  $\alpha$ -functionalization of different enamines in presence of methyl malonate, methyl acetoacetate or acetylacetone **158** (Scheme 45). Depending on the employed enamine **157**, the applied oxidation potential led to the formation of the desired products **159**. Enamines derived from cyclopentanone (**157** with  $n=0$ ) were more easily oxidized than the corresponding six members homologues. At the same time, pyrrolidine-adducts were oxidizable at more cathodic potentials than those of the corresponding piperidine or morpholine enamines. An excess of methyl acetoacetate was employed in order to disfavor the methoxylation process. The electrochemistry was performed in an H-type cell, equipped with a glass frit



**Scheme 44.** Electrooxidation of enamines in methanol.



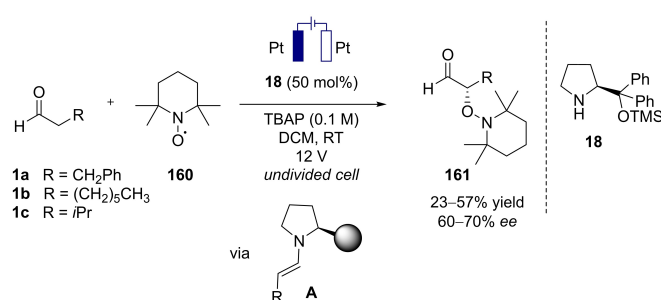
**Scheme 45.**  $\alpha$ -Functionalization of different enamines with dicarbonyl compounds.

diaphragm to separate the two compartments. The anodic cell was equipped with a Pt plate and a stirring bar, while the cathodic cell contained a Pt wire.<sup>[92]</sup> Upon the delivery of a constant current of 0.5 A versus the SCE, the final products could be isolated within yields ranging from 29 to 67%. The yields were significantly influenced by the oxidation potential of enamines. Higher potential was detrimental for the transformation. The electrochemical oxidation of enamines in presence of other reagents largely relays on the stability of the enamines in oxidative conditions and on their basicity. Indeed, the higher basicity enhances the formation of iminium cations at the cathode, hampering the reaction outcome.

### 5.3. Enamine-electro synergistic catalysis

In the context of oxidized enamine radical-mediated transformations, Jang and co-workers reported the enantioselective  $\alpha$ -substitution of aldehydes **1** with TEMPO, in presence of a chiral secondary amine as a catalyst.<sup>[93]</sup> Enamine intermediate **A** exhibits an electrochemically irreversible redox pattern at the platinum electrode. In the range 0.0 to 2.0 V, two oxidation waves appeared at  $E = +0.71$  and  $+0.95$  V, which are assumed to be the cationic radical ( $3\pi e^-$ ) and the allylic cation, respectively. Exploiting the cyclic voltammetry and control experiments, the authors underlined that the enamine-radical-mediated reaction is possible by an anodic oxidation. The electrochemical organocatalyzed  $\alpha$ -oxyamination of aldehydes was conducted in an undivided cell, developing an observed current value of 12 V, in presence of TBAP as supporting electrolyte and involving 0.5 equivalents of the chiral Jørgensen/Hayashi catalyst **18**. With the optimized conditions in hand, the reaction was performed on hydrocinnamaldehyde (**1a**), octanal (**1b**) and isovaleraldehyde (**1c**) providing the corresponding coupling products **161** with TEMPO **160** in 57, 23 and 49% isolated yields and 64, 70 and 60% ee, respectively (Scheme 46).

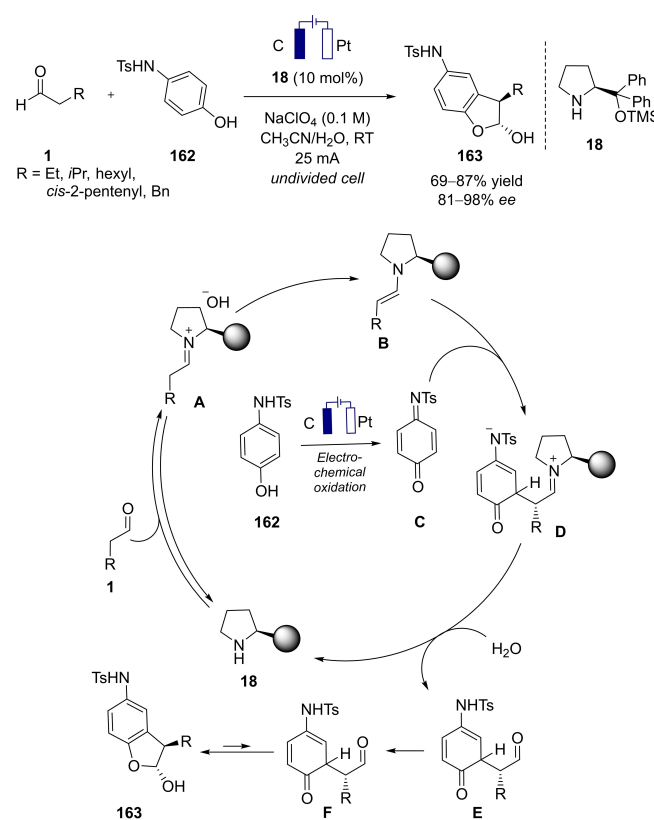
One year later, Jørgensen et al. developed an electro-mediated enantioselective synthesis of benzofuranes from the condensation between *para*-hydroxy-*N*-tosyl anilines **162** and aliphatic aldehydes, in presence of **18** under electrochemical conditions.<sup>[94]</sup> The reaction was conducted in undivided cells with  $\text{NaClO}_4$  as supporting electrolyte. Carbon and platinum rods were used respectively as anode and cathode materials. The anodic oxidation was carried out with an applied constant current of 25 mA under galvanostatic conditions. This protocol



**Scheme 46.**  $\alpha$ -Oxyamination of aldehydes through enamine/electro synergistic catalysis.

allowed the preparation of the corresponding desired heterocycles **163** with isolated yields ranging from 69 to 87% and excellent ee (from 81 to 98%). From a mechanistic standpoint, the electricity is supposed to help the formation of the proper unpoled electrophilic aromatic partner **C** through an electro-mediated oxidation event. Such species are further trapped by the nucleophilic enamine **B**, generated in situ upon reaction between the organocatalyst and the aldehyde (Scheme 47).

The same year, Jang and co-workers developed an enantioselective electrochemical procedure for the coupling of aldehydes **1** and xantene **164** under galvanostatic conditions.<sup>[95]</sup> The desired transformation was performed in presence of

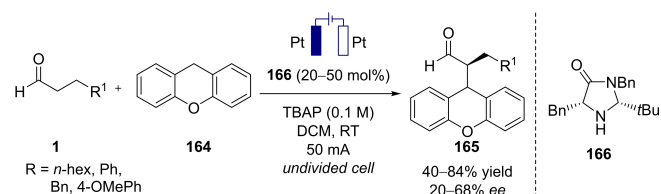


**Scheme 47.** Stereoselective  $\alpha$ -arylation/hemiacetalization of aldehydes through enamine/electro synergistic catalysis.

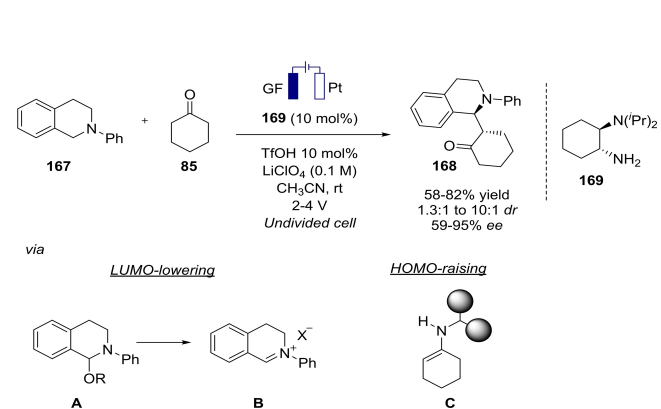
50 mol% of the chiral catalyst **166**. Two equivalents of xantene per equivalent of hydrocinnamaldehyde were stirred in an undivided cell in dichloromethane in presence of TBAP as electrolyte, with a constant current value of 50 mA and platinum gauze as both anode and cathode material. Albeit the absence of reference electrode at the end of the reaction, a significant increase of the potential was observed, leading to the formation of the desired product **165** with a 43% isolated yield and promising *ee* (Scheme 48).

C–H functionalization has emerged as one of the most studied organic transformations. As well, greener and more sustainable approaches are nowadays deeply investigated as powerful alternatives to the use of toxic and expensive metals and chemical oxidants.<sup>[96]</sup> As well, the cross-dehydrogenative coupling represents one of the most investigated processes, being a straightforward opportunity to build new C–C bonds. In 2017, Luo and co-workers reported a first electrochemical C–H oxidation combined HOMO-raising activations of ketones **85** for a formal asymmetric synthesis of *N*-aryl  $\gamma$ -amino carbonyl derivatives **168** (Scheme 49).<sup>[97]</sup>

Presumably, the formation of an unstable iminium ion intermediate **B** could lead to the formation of adducts on the electrode surface, not effectively captured by the enamine intermediate **C**. To overcome this issue, the addition of proton sources such as trifluoroethanol and 2,6-lutidine resulted crucial to enhance the reaction rate,<sup>[98]</sup> stabilizing hemiaminal **A** formed in situ and, at the same time, favoring the cathodic reduction of molecular hydrogen, increasing the conductivity. The electrochemistry was performed into undivided cells equipped with graphite and platinum at anode and cathode respectively, in presence of LiClO<sub>4</sub> as electrolyte. The experiments were run at a



**Scheme 48.** Enantioselective enamine-/electrochemically driven coupling of aldehydes with xantene.

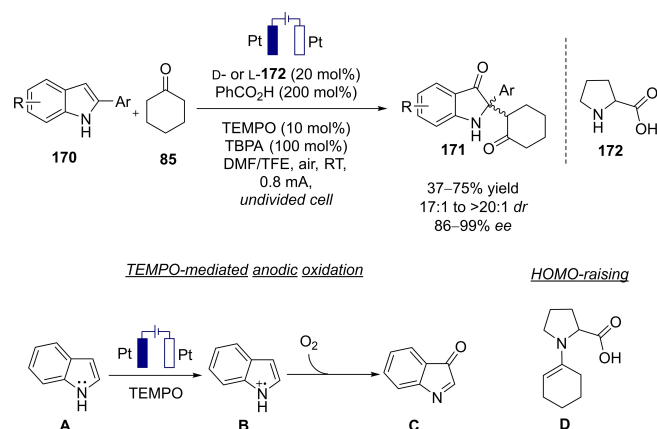


**Scheme 49.** Asymmetric  $\alpha$ -alkylation of ketones by synergistic combination of amino- and electro-catalysis C–H functionalization of ketones.

potential of 3.0 V. With the optimized conditions, a series of different  $\alpha$ -alkylated ketones **168** were effectively prepared within yields from 58 to 82% and good to high *ee* from 59 to 95%, with diastereoselectivities ranging from 1.3:1 to 7:1. In the same year, an analogue reaction was performed by the same group through photoredox-assisted reduction of **167** by means of Ru<sup>II</sup> and Co<sup>III</sup> catalysis.<sup>[99]</sup>

In 2020, He and co-workers discovered a procedure for a highly enantioselective synthesis of 2-substituted arylindolin-3-ones **171** (Scheme 50).<sup>[100]</sup> First attempts have been made using cyclohexanone **85** as a partner and conducted in an undivided cell setup. After an optimization consisting of an ample screening of solvents, electrolytes and mediators, the optimal conditions could provide the final product within 67% yield and 98% *ee*. The use of proline **172** ensured high enantioselectivities, while the electrochemistry was performed in presence of platinum at both anode and cathode, in presence of TBPA as electrolyte in DMF/TFE mixture, under air, within constant current conditions (0.8 mA). The addition of catalytic amounts of TEMPO as redox mediator resulted in an improvement in the isolated yield from 50 to 67%, regardless the enantioselectivity. A large variety of substrates underwent electrolysis with the established conditions, providing the desired products **171** within 37 to 75% isolated yield and high *ee*.

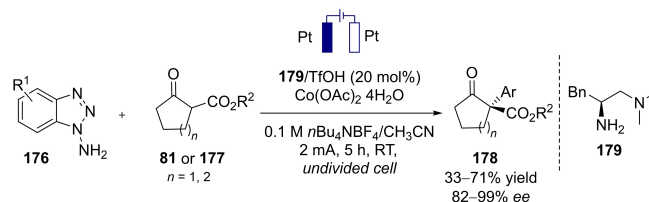
Huang and co-workers proposed an electrochemical 3-functionalization of indoles **173**, leading to the synthesis of formylated products **175**, starting from glyoxylic acid **174**.<sup>[101]</sup> The initial reaction attempts have been performed in undivided cell. Platinum was used as anode and cathode, and the electrochemistry performed at 5 mA, under constant current conditions in DMSO at room temperature. For the optimization, different amines were screened, and as a general trend, the efficiency of the transformation was higher when their nucleophilicity and oxidation potential were higher. As a consequence, dimethylamine and aniline were found to be the best candidates, able to provide the desired formylation product **175** within higher yields. More oxidation-sensitive substrates bearing chlorine and bromine moieties, could be



**Scheme 50.** Synthesis of quaternary indolin-3-ones.

obtained in good yields (73 and 89% respectively). On the other side, the presence of electron-donating groups was highly tolerated in presence of both the amines. Control experiments suggested that the process could presumably take place thanks to the formation of iminium ion **A** through the condensation of the aminocatalyst with the glyoxylate. The authors suggested two plausible pathways after the generation of open-shell radical species **B**. Following path 1, this intermediate may be intercepted by the nucleophilic *N*-methylindole **173** after losing a second electron, affording the iminium ion **C**. The formylated product **175** is then generated after hydrolysis. Alternatively, a radical path 2 might take place to give the  $10e^-$  intermediate **D** instead.

In 2020, Luo and co-workers developed an asymmetric arylation of oxo-cyclohexane carboxylate derivatives under electrochemical conditions (Scheme 51). The key step of the transformation was the generation of a benzyne intermediate at the anode upon oxidation of 1-aminobenzotriazole **176** ( $E_{1/2}^{ox} = +0.84$  V), an alternative reagent to the typical Kobayashi benzyne precursor (2-(trimethylsilyl)phenyl triflate). The reaction proceeded smoothly in undivided cell in presence of platinum at both cathode and anode. The electrochemistry was performed under constant current conditions (2 mA). The employ of cobalt acetate as additive was found to be beneficial to the final reaction outcome, being presumably capable of stabilizing the benzyne generated in situ. The chiral primary amine catalyst **179** ( $E_{1/2}^{ox} = +1.54$  V) could not be oxidized under the estab-



**Scheme 52.**  $\alpha$ -Arylation of  $\alpha$ -branched ketones by means of synergistic use of aminocatalysis and electrochemistry.

lished conditions, reacting with the carbonyl compound (**81** or **177**) to generate the corresponding enamine, able to trap the benzyne. With the optimized conditions, a large cohort of asymmetric  $\alpha$ -substituted  $\beta$ -ketoester derivatives **178** could be isolated with yields from 33 to 71% and excellent enantioselectivities (82 to 99%; Scheme 52).<sup>[102]</sup>

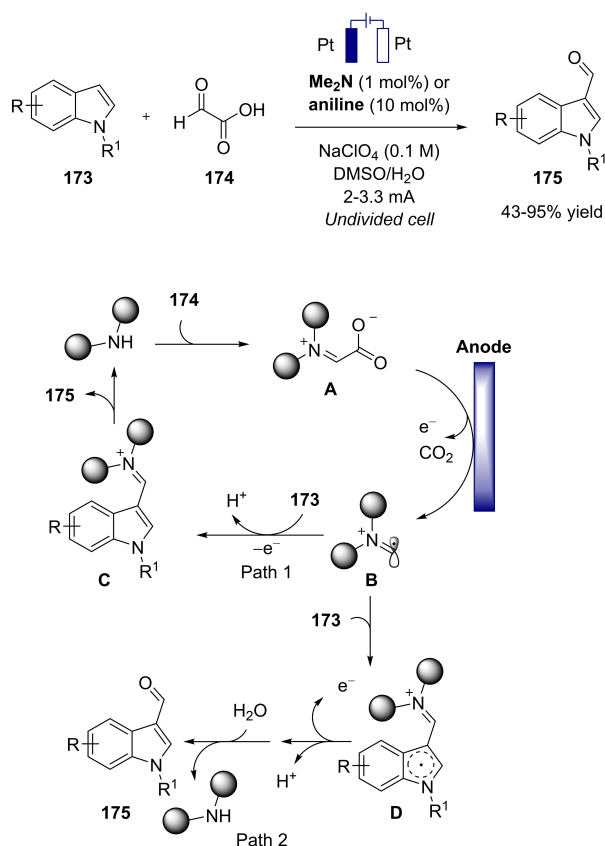
Due to the encountered problematics of overoxidation combined with the danger of low enantioselectivities and functional group tolerance, the synergy of electro and amino catalysis still remains a less developed arena. However, the recent applications of electrochemistry on organic synthesis, offer large perspectives of improvements, furnishing, at the same time, more and more powerful tools for the establishment of solid protocols to pursue an extensive array of transformations.

## 6. General Remarks and Conclusions

From the beginning of this century, we have taken part in the renaissance of organocatalysis driven by the development of asymmetric aminocatalysis. Recently, researchers have been attracted by the tremendous potential of this synthetic paradigm in combination with organo-, metal, photoredox, and electrocatalysis. Synergistic applications of aminocatalysis are fast expanding, setting up new synthetic concepts. On the other hand, this exciting area is still mostly focused on the mother activation intermediates: enamine and iminium-ion. Engineering the privileged chiral amines, the scientific community has already tackled some of the major challenges, charting a course for exploiting the whole potential of HOMO-raising and LUMO-lowering activation of carbonyl compounds in synergistic aminocatalysis.

## Acknowledgements

F.P. thanks PON-AIM1842894, CUP-E18D19000560001, for funding this research. G.G. is grateful to PON-DOT13OV20C for an industrial PhD fellowship. Open Access funding provided by Università degli Studi dell'Aquila within the CRUI-CARE Agreement.



**Scheme 51.** Electrochemical 3-functionalization of indoles.



## Conflict of Interest

The authors declare no conflict of interest.

## Data Availability Statement

The data that support the findings of this study are available from the corresponding author upon reasonable request.

**Keywords:** aminocatalysis · asymmetric catalysis · electrocatalysis · organocatalysis · photoredox catalysis · synergistic catalysis

- [1] a) B. List, R. A. Lerner, C. F. Barbas, *J. Am. Chem. Soc.* **2000**, *122*, 2395–2396; b) K. A. Ahrendt, C. J. Borths, D. W. C. MacMillan, *J. Am. Chem. Soc.* **2000**, *122*, 4243–4244.
- [2] For reviews on asymmetric aminocatalysis see: a) B. Han, X.-H. He, Y.-Q. Liu, G. He, C. Peng, J.-L. Li, *Chem. Soc. Rev.* **2021**, *50*, 1522–1586; b) E. Juaristi, *Tetrahedron* **2021**, *88*, 132143; c) H. Jiang, Ł. Albrecht, K. A. Jørgensen, *Chem. Sci.* **2013**, *4*, 2287–2300; d) P. Melchiorre, *Angew. Chem. Int. Ed.* **2012**, *51*, 9748–9770; *Angew. Chem.* **2012**, *124*, 9886–9909; e) C. Grondal, M. Jeanty, D. Enders, *Nat. Chem.* **2010**, *2*, 167–178; f) S. Bertelsen, K. A. Jørgensen, *Chem. Soc. Rev.* **2009**, *38*, 2178–2189; g) P. Melchiorre, M. Marigo, A. Carlone, G. Bartoli, *Angew. Chem. Int. Ed.* **2008**, *47*, 6138–6171; *Angew. Chem.* **2008**, *120*, 6232–6265; h) A. Erkkilä, I. Majander, P. M. Pihko, *Chem. Rev.* **2007**, *107*, 5416–5470; i) B. List, *Chem. Rev.* **2007**, *107*, 5413–5415; j) S. Mukherjee, J. W. Yang, S. Hoffmann, B. List, *Chem. Rev.* **2007**, *107*, 5471–5569; k) B. List, *Chem. Commun.* **2006**, 819–824; l) J. Seayad, B. List, *Org. Biomol. Chem.* **2005**, *3*, 719–724.
- [3] For reviews on multicyclic catalysis involving organocatalysts see: a) X. Xiao, B.-X. Shao, Y.-J. Lu, Q.-Q. Cao, C.-N. Xia, F.-E. Chen, *Adv. Synth. Catal.* **2021**, *363*, 352–387; b) A. Sinibaldi, V. Nori, A. Baschieri, F. Fini, A. Arcadi, A. Carlone, *Catal.* **2019**, *9*, 928–962; c) G. Jindal, H. K. Kisan, R. B. Sunoj, *ACS Catal.* **2015**, *5*, 480–503; d) A. E. Allen, D. W. C. MacMillan, *Chem. Sci.* **2012**, *3*, 633–658. For selected reports on synergistic catalysis involving aminocatalysis prior to 2015 see: e) X. Yang, R. J. Phipps, F. D. Toste, *J. Am. Chem. Soc.* **2014**, *136*, 5225–5228; f) S. Muramulla, J.-A. Ma, J. C.-G. Zhao, *Adv. Synth. Catal.* **2013**, *355*, 1260–1264; g) N. Z. Burns, M. R. Witten, E. N. Jacobsen, *J. Am. Chem. Soc.* **2011**, *133*, 14578–14581; h) Z.-B. Li, S.-P. Luo, Y. Guo, A.-B. Xia, D.-Q. Xu, *Org. Biomol. Chem.* **2010**, *8*, 2505–2508; i) Z.-B. Li, S.-P. Luo, Y. Guo, A.-B. Xia, D.-Q. Xu, *Org. Biomol. Chem.* **2010**, *8*, 2505–2508; j) A.-B. Xia, D.-Q. Xu, S.-P. Luo, J.-R. Jiang, Y.-F. Wang, Z.-Y. Xu, *Chem. Eur. J.* **2010**, *16*, 801–804; k) S. P. Lathrop, T. Rovis, *J. Am. Chem. Soc.* **2009**, *131*, 13628–13630; l) T. Mandal, C.-G. Zhao, *Angew. Chem. Int. Ed.* **2008**, *47*, 7714–7717; *Angew. Chem.* **2008**, *120*, 7828–7831.
- [4] For non synergistic enantioselective  $\alpha$ -alkylation of aldehydes by HOMO-raising see: a) B. List, I. Čorić, O. O. Grygorenko, P. S. J. Kaib, I. Komarov, A. Lee, M. Leutzsch, S. Chandra Pan, A. V. Tytmsunik, M. van Gemmeren, *Angew. Chem. Int. Ed.* **2014**, *53*, 282–285; *Angew. Chem.* **2014**, *126*, 286–289; b) N. Vignola, B. List, *J. Am. Chem. Soc.* **2004**, *126*, 450–451.
- [5] P. G. Cozzi, F. Benfatti, L. Zoli, *Angew. Chem. Int. Ed.* **2009**, *48*, 1313–1316; *Angew. Chem.* **2009**, *121*, 1339–1342.
- [6] G. Bergonzini, S. Vera, P. Melchiorre, *Angew. Chem. Int. Ed.* **2010**, *49*, 9685–9688; *Angew. Chem.* **2010**, *122*, 9879–9882.
- [7] a) M. S. Kutwal, V. M. D. Padmaja, C. Appayee, *Eur. J. Org. Chem.* **2020**, *2020*, 2720–2724; b) V. M. D. Padmaja, S. Jangra, C. Appayee, *Org. Biomol. Chem.* **2019**, *17*, 1714–1717; c) M. S. Kutwal, C. Appayee, *Eur. J. Org. Chem.* **2017**, *2017*, 4230–4234; d) M. Silvi, C. Cassani, A. Moran, P. Melchiorre, *Helv. Chim. Acta* **2012**, *95*, 1985–2006; e) J. Stiller, E. Marqués-López, R. P. Herrera, R. Fröhlich, C. Strohmann, M. Christmann, *Org. Lett.* **2011**, *13*, 70–73.
- [8] J. Song, C. Guo, A. Adele, H. Yin, L.-Z. Gong, *Chem. Eur. J.* **2013**, *19*, 3319–3323.
- [9] S. Wang, X. Li, H. Liu, L. Xu, J. Zhuang, J. Li, H. Li, W. Wang, *J. Am. Chem. Soc.* **2015**, *137*, 2303–2310.
- [10] J. Chen, Y. Fu, Y. Yu, J.-R. Wang, Y.-W. Guo, H. Li, W. Wang, *Org. Lett.* **2020**, *22*, 6061–6066.
- [11] J.-B. Lu, C.-H. Shi, D. Hu, X.-Y. Gao, Z.-C. Chen, W. Du, Y.-C. Chen, *Org. Lett.* **2021**, *23*, 145–149.
- [12] X. Mo, D. G. Hall, *J. Am. Chem. Soc.* **2016**, *138*, 10762–10765.
- [13] a) C. Xu, L. Zhang, S. Luo, *Angew. Chem. Int. Ed.* **2014**, *53*, 4149–4153; *Angew. Chem.* **2014**, *126*, 4233–4237; b) H. Zhou, L. Zhang, C. Xu, S. Luo, *Angew. Chem. Int. Ed.* **2015**, *54*, 12645–12648; *Angew. Chem.* **2015**, *127*, 12836–12839; c) Q. Yang, L. Zhang, C. Ye, S. Luo, L.-Z. Wu, C.-H. Tung, *Angew. Chem. Int. Ed.* **2017**, *56*, 3694–3698; *Angew. Chem.* **2017**, *129*, 3748–3752; d) L. Zhu, L. Zhang, S. Luo, *Angew. Chem. Int. Ed.* **2018**, *57*, 2253–2258; *Angew. Chem.* **2018**, *130*, 2275–2280; e) Y. Wang, H. Zhou, K. Yang, C. You, L. Zhang, S. Luo, *Org. Lett.* **2019**, *21*, 407–411; f) M. Cai, K. Xu, Y. Li, Z. Nie, L. Zhang, S. Luo, *J. Am. Chem. Soc.* **2021**, *143*, 1078–1087.
- [14] Q. Zhang, Y. Li, L. Zhang, S. Luo, *Angew. Chem. Int. Ed.* **2021**, *60*, 10971–10976; *Angew. Chem.* **2021**, *133*, 11066–11071.
- [15] a) E. Jafari, P. Chauhan, M. Kumar, X.-Y. Chen, S. Li, C. von Essen, K. Rissanen, D. Enders, *Eur. J. Org. Chem.* **2018**, *2018*, 2462–2465; b) A. Raja, B.-C. Hong, G.-H. Lee, *Org. Lett.* **2014**, *16*, 5756–5759; c) L. Dell'Amico, Ł. Albrecht, T. Naicker, P. H. Poulsen, K. A. Jørgensen, *J. Am. Chem. Soc.* **2013**, *135*, 8063–8070; d) S. Duce, A. Mateo, I. Alonso, J. L. García Ruano, M. B. Cid, *Chem. Commun.* **2012**, *48*, 5184–5186; e) S. Hanessian, V. Pham, *Org. Lett.* **2000**, *2*, 2975–2978.
- [16] G. Rassu, C. Curti, V. Zambrano, L. Pinna, N. Brindani, G. Pelosi, F. Zanardi, *Chem. Eur. J.* **2016**, *22*, 12637–12640.
- [17] S. Lin, L. Deiana, G.-L. Zhao, J. Sun, A. Córdova, *Angew. Chem. Int. Ed.* **2011**, *50*, 7624–7630; *Angew. Chem.* **2011**, *123*, 7766–7772.
- [18] L. Prieto, V. Juste-Navarro, U. Uria, I. Delso, E. Reyes, T. Tejero, L. Carrillo, P. Merino, J. L. Vicario, *Chem. Eur. J.* **2017**, *23*, 2764–2768.
- [19] C. Wang, Y.-H. Chen, H.-C. Wu, C. Wang, Y.-K. Liu, *Org. Lett.* **2019**, *21*, 6750–6755.
- [20] H.-C. Wu, C. Wang, Y.-H. Chen, Y.-K. Liu, *Chem. Commun.* **2021**, *57*, 1762–1765.
- [21] For selected examples on differentiating catalysis see: a) D. McLeod, J. A. Izzo, D. K. B. Jørgensen, R. F. Lauridsen, K. A. Jørgensen, *ACS Catal.* **2020**, *10*, 10784–10793; b) C. Curti, G. Rassu, M. Lombardo, V. Zambrano, L. Pinna, L. Battistini, A. Sartori, G. Pelosi, F. Zanardi, *Angew. Chem. Int. Ed.* **2020**, *59*, 20055–20064; *Angew. Chem.* **2020**, *132*, 20230–20239.
- [22] A. Topolska, S. Frankowski, Ł. Albrecht, *Org. Lett.* **2022**, *24*, 955–959.
- [23] M. Cai, K. Xu, Y. Li, Z. Nie, L. Zhang, S. Luo, *J. Am. Chem. Soc.* **2021**, *143*, 1078–1087.
- [24] S. Afewerki, A. Córdova, *Chem. Rev.* **2016**, *116*, 13512–13570.
- [25] P. G. Cozzi, A. Gualandi, S. Potenti, F. Calogero, G. Rodeghiero, *Top. Curr. Chem.* **2019**, *378*, 1.
- [26] a) I. Ibrahim, A. Córdova, *Angew. Chem. Int. Ed.* **2006**, *45*, 1952–1956; *Angew. Chem.* **2006**, *118*, 1986–1990; b) S. Afewerki, I. Ibrahim, J. Rydfjord, P. Breistein, A. Córdova, *Chem. Eur. J.* **2012**, *18*, 2972–2977.
- [27] C. Defieber, M. A. Ariger, P. Moriel, E. M. Carreira, *Angew. Chem. Int. Ed.* **2007**, *46*, 3139–3143; *Angew. Chem.* **2007**, *119*, 3200–3204.
- [28] S. Krautwald, D. Sarlah, M. A. Schafroth, E. M. Carreira, *Science* **2013**, *340*, 1065–1068.
- [29] S. Krautwald, M. A. Schafroth, D. Sarlah, E. M. Carreira, *J. Am. Chem. Soc.* **2014**, *136*, 3020–3023.
- [30] T. Sandmeier, S. Krautwald, H. F. Zipfel, E. M. Carreira, *Angew. Chem. Int. Ed.* **2015**, *54*, 14363–14367; *Angew. Chem.* **2015**, *127*, 14571–14575.
- [31] F. A. Cruz, V. M. Dong, *J. Am. Chem. Soc.* **2017**, *139*, 1029–1032.
- [32] For other selected examples reported by the same group on amino-metal synergistic catalysis employing  $\beta$ -keto esters see also: a) X. Xie, L. Zhang, Q. He, J. Hou, C. Xu, N. Zhang, S. Luo, Z. Nie, *Chem. Eur. J.* **2015**, *21*, 14630–14637; b) C. Xu, L. Zhang, S. Luo, *Angew. Chem. Int. Ed.* **2014**, *53*, 4149–4153; *Angew. Chem.* **2014**, *126*, 4233–4237.
- [33] J. Zhang, Y. Wang, C. You, M. Shi, X. Mi, S. Luo, *Org. Lett.* **2022**, *24*, 1186–1189.
- [34] H. Zhou, L. Zhang, C. Xu, S. Luo, *Angew. Chem. Int. Ed.* **2015**, *54*, 12645–12648; *Angew. Chem.* **2015**, *127*, 12836–12839.
- [35] M. Li, S. Datta, D. M. Barber, D. J. Dixon, *Org. Lett.* **2012**, *14*, 6350–6353.
- [36] A. Ballesteros, P. Morán-Poladura, J. M. González, *Chem. Commun.* **2016**, *52*, 2905–2908.
- [37] J. Fernández-Casado, R. Nelson, J. L. Mascareñas, F. López, *Chem. Commun.* **2016**, *52*, 2909–2912.
- [38] H. Zhou, Y. Wang, L. Zhang, M. Cai, S. Luo, *J. Am. Chem. Soc.* **2017**, *139*, 3631–3634.

- [39] A. Leitner, J. Larsen, C. Steffens, J. F. Hartwig, *J. Org. Chem.* **2004**, *69*, 7552–7557.
- [40] Y. Wang, J. Zhang, C. You, X. Mi, S. Luo, *CCS* **2021**, *3*, 2622–2630.
- [41] Y.-N. Xu, M.-Z. Zhu, S.-K. Tian, *J. Org. Chem.* **2019**, *84*, 14936–14942.
- [42] H.-C. Shen, L. Zhang, S.-S. Chen, J. Feng, B.-W. Zhang, Y. Zhang, X. Zhang, Y.-D. Wu, L.-Z. Gong, *ACS Catal.* **2019**, *9*, 791–797.
- [43] C. Wei, X. Ye, Q. Xing, Y. Hu, Y. Xie, X. Shi, *Org. Biomol. Chem.* **2019**, *17*, 6607–6611.
- [44] Y. Wang, J. Chai, C. You, J. Zhang, X. Mi, L. Zhang, S. Luo, *J. Am. Chem. Soc.* **2020**, *142*, 3184–3195.
- [45] H. Wang, R. Zhang, Q. Zhang, W. Zi, *J. Am. Chem. Soc.* **2021**, *143*, 10948–10962.
- [46] M. Mahlau, B. List, *Angew. Chem. Int. Ed.* **2013**, *52*, 518–533; *Angew. Chem.* **2013**, *125*, 540–556.
- [47] S. Mukherjee, B. List, *J. Am. Chem. Soc.* **2007**, *129*, 11336–11337.
- [48] Á. M. Pálvölgyi, J. Smith, M. Schnürch, K. Bica-Schröder, *J. Org. Chem.* **2021**, *86*, 850–860.
- [49] a) M. Meazza, M. E. Light, A. Mazzanti, R. Rios, *Chem. Sci.* **2016**, *7*, 984–988; b) M. Meazza, V. Polo, P. Merino, R. Rios, *Org. Chem. Front.* **2018**, *5*, 806–812. For other selected examples from the same group see; c) S. Putatunda, J. V. Alegre-Requena, M. Meazza, M. Franc, D. Rohal'ová, P. Vemuri, I. Císařová, R. P. Herrera, R. Rios, J. Veselý, *Chem. Sci.* **2019**, *10*, 4107–4115; d) M. Meazza, G. Sotinova, C. Poderi, M. Mancinelli, K. Zhang, A. Mazzanti, R. R. Torres, *Chem. Eur. J.* **2018**, *24*, 13306–13310; e) K. Zhang, M. Meazza, A. Izaga, C. Contamine, M. C. Gimeno, R. P. Herrera, R. Rios, *Synthesis (Stuttg.)* **2017**, *49*, 167–174.
- [50] a) M. Franc, I. Císařová, J. Veselý, *Adv. Synth. Catal.* **2021**, *363*, 4349–4353; b) M. Kamlar, M. Franc, I. Císařová, R. Gyepes, J. Veselý, *Chem. Commun.* **2019**, *55*, 3829–3832.
- [51] A. E. Allen, D. W. C. MacMillan, *J. Am. Chem. Soc.* **2011**, *133*, 4260–4263.
- [52] For reviews on photoredox catalysis see: a) P. Melchiorre, *Chem. Rev.* **2022**, *122*, 1483–1484; b) M. J. Genzink, J. B. Kidd, W. B. Swords, T. P. Yoon, *Chem. Rev.* **2022**, *122*, 1654–1716; c) A. Y. Chan, I. B. Perry, N. B. Bissonnette, B. F. Buksh, G. A. Edwards, L. I. Frye, O. L. Garry, M. N. Lavagnino, B. X. Li, Y. Liang, E. Mao, A. Millet, J. V. Oakley, N. L. Reed, H. A. Sakai, C. P. Seath, D. W. C. MacMillan, *Chem. Rev.* **2022**, *122*, 1485–1542; d) G. E. M. Crisenza, D. Mazzarella, P. Melchiorre, *J. Am. Chem. Soc.* **2020**, *142*, 5461–5476; e) C. Prentice, J. Morrisson, A. D. Smith, E. Zysman-Colman, *Beilstein J. Org. Chem.* **2020**, *16*, 2363–2441; f) Y.-Q. Zou, F. M. Hörmann, T. Bach, *Chem. Soc. Rev.* **2018**, *47*, 278–290; g) M. Silvi, P. Melchiorre, *Nature* **2018**, *554*, 41–49; h) M. H. Shaw, J. Twilton, D. W. C. MacMillan, *J. Org. Chem.* **2016**, *81*, 6898–6926; i) M. A. Cismesia, T. P. Yoon, *Chem. Sci.* **2015**, *6*, 5426–5434.
- [53] For review on amino/photoredox catalysis see: a) A. Gualandi, P. G. Cozzi, G. Rodeghiero, T. P. Jansen, R. Perciaccante, *Phys. Sci. Rev.* **2020**, *5*, 20180098–20180120.
- [54] T. D. Beeson, A. Mastracchio, J.-B. Hong, K. Ashton, D. W. C. MacMillan, *Science* **2007**, *316*, 582–585.
- [55] a) M. P. Sibi, M. Hasegawa, *J. Am. Chem. Soc.* **2007**, *129*, 4124–4125; b) J. F. Van Humbeck, S. P. Simonovich, R. R. Knowles, D. W. C. MacMillan, *J. Am. Chem. Soc.* **2010**, *132*, 10012–10014.
- [56] D. A. Nicewicz, D. W. C. MacMillan, *Science* **2008**, *322*, 77–80.
- [57] M. A. Cismesia, T. P. Yoon, *Chem. Sci.* **2015**, *6*, 5426–5434.
- [58] H.-W. Shih, M. N. Vander Wal, R. L. Grange, D. W. C. MacMillan, *J. Am. Chem. Soc.* **2010**, *132*, 13600–13603.
- [59] E. R. Welin, A. A. Warkentin, J. C. Conrad, D. W. C. MacMillan, *Angew. Chem. Int. Ed.* **2015**, *54*, 9668–9672; *Angew. Chem.* **2015**, *127*, 9804–9808.
- [60] D. A. Nagib, M. E. Scott, D. W. C. MacMillan, *J. Am. Chem. Soc.* **2009**, *131*, 10875–10877.
- [61] a) T. Rigotti, A. Casado-Sánchez, S. Cabrera, R. Pérez-Ruiz, M. Liras, V. A. de la Peña O'Shea, J. Alemán, *ACS Catal.* **2018**, *8*, 5928–5940; b) M. Neumann, S. Földner, B. König, K. Zeitler, *Angew. Chem. Int. Ed.* **2011**, *50*, 951–954; *Angew. Chem.* **2011**, *123*, 981–985.
- [62] M. Cherevatskaya, M. Neumann, S. Földner, C. Harlander, S. Kümmel, S. Dankesreiter, A. Pfitzner, K. Zeitler, B. König, *Angew. Chem. Int. Ed.* **2012**, *51*, 4062–4066; *Angew. Chem.* **2012**, *124*, 4138–4142.
- [63] a) A. Gualandi, M. Marchini, L. Mengozzi, H. T. Kidanu, A. Franc, P. Ceroni, P. G. Cozzi, *Eur. J. Org. Chem.* **2020**, *2020*, 1486–1490; b) A. Gualandi, M. Marchini, L. Mengozzi, M. Natali, M. Lucarini, P. Ceroni, P. G. Cozzi, *ACS Catal.* **2015**, *5*, 5927–5931.
- [64] Y. Zhu, L. Zhang, S. Luo, *J. Am. Chem. Soc.* **2014**, *136*, 14642–14645.
- [65] a) G. E. M. Crisenza, D. Mazzarella, P. Melchiorre, *J. Am. Chem. Soc.* **2020**, *142*, 5461–5476; b) S. V. Rosokha, J. K. Kochi, *Acc. Chem. Res.* **2008**, *41*, 641–653.
- [66] E. Arceo, I. D. Jurberg, A. Álvarez-Fernández, P. Melchiorre, *Nat. Chem.* **2013**, *5*, 750–756.
- [67] A. Bahamonde, P. Melchiorre, *J. Am. Chem. Soc.* **2016**, *138*, 8019–8030.
- [68] a) A. G. Capacci, J. T. Malinowski, N. J. McAlpine, J. Kuhne, D. W. C. MacMillan, *Nat. Chem.* **2017**, *9*, 1073–1077.
- [69] M. Silvi “New Directions in Aminocatalysis: Vinylogy and Photochemistry” TDX (Tesis Doctorals en Xarxa), Universitat Rovira i Virgili, **2015**.
- [70] M. Silvi, E. Arceo, I. D. Jurberg, C. Cassani, P. Melchiorre, *J. Am. Chem. Soc.* **2015**, *137*, 6120–6123.
- [71] G. Filippini, M. Silvi, P. Melchiorre, *Angew. Chem. Int. Ed.* **2017**, *56*, 4447–4451; *Angew. Chem.* **2017**, *129*, 4518–4522.
- [72] a) J. A. Terrett, M. D. Clift, D. W. C. MacMillan, *J. Am. Chem. Soc.* **2014**, *136*, 6858–6861; b) F. R. Petronijević, M. Nappi, D. W. C. MacMillan, *J. Am. Chem. Soc.* **2013**, *135*, 18323–18326; c) M. T. Pirnot, D. A. Rankic, D. B. C. Martin, D. W. C. MacMillan, *Science* **2013**, *340*, 1593–1596.
- [73] J. S. DeHovitz, Y. Y. Loh, J. A. Kautzky, K. Nagao, A. J. Meichan, M. Yamauchi, D. W. C. MacMillan, T. K. Hyster, *Science* **2020**, *369*, 1113–1118.
- [74] W. W. Schoeller, J. Niemann, P. Rademacher, *J. Chem. Soc. Perkin Trans. 2* **1988**, 369–373.
- [75] a) A. Hözl-Hobmeier, A. Bauer, A. V. Silva, S. M. Huber, C. Bannwarth, T. Bach, *Nature* **2018**, *564*, 240–243; b) M. Plaza, C. Jandl, T. Bach, *Angew. Chem. Int. Ed.* **2020**, *59*, 12785–12788; *Angew. Chem.* **2020**, *132*, 12885–12888.
- [76] N. Y. Shin, J. M. Ryss, X. Zhang, S. J. Miller, R. R. Knowles, *Science* **2019**, *366*, 364–369.
- [77] M. Huang, L. Zhang, T. Pan, S. Luo, *Science* **2022**, *375*, 869–874.
- [78] B. Schweitzer-Chaput, M. A. Horwitz, E. de Pedro Beato, P. Melchiorre, *Nat. Chem.* **2019**, *11*, 129–135.
- [79] In the Giese reactions the authors employed  $\gamma$ -terpinene as donor of H<sup>•</sup> and electrons. J. Davies, T. D. Svejstrup, D. Fernandez Reina, N. S. Sheikh, D. Leonori, *J. Am. Chem. Soc.* **2016**, *138*, 8092–8095.
- [80] D. Spinnato, B. Schweitzer-Chaput, G. Goti, M. Ošeka, P. Melchiorre, *Angew. Chem. Int. Ed.* **2020**, *59*, 9485–9490; *Angew. Chem.* **2020**, *132*, 9572–9577.
- [81] For selected examples of iminium ion activation in photocatalysis see: a) A. M. Martínez-Gualda, P. Domingo-Legarda, T. Rigotti, S. Díaz-Tendero, A. Fraile, J. Alemán, *Chem. Commun.* **2021**, *57*, 3046–3049; b) F. Pecho, Y. Sempere, J. Gramüller, F. M. Hörmann, R. M. Gschwind, T. Bach, *J. Am. Chem. Soc.* **2021**, *143*, 9350–9354.
- [82] H. J. Jakobsen, S.-O. Lawesson, J. T. B. Marshall, G. Schroll, D. H. Williams, *J. Chem. Soc. B* **1966**, 940–946.
- [83] J. J. Murphy, D. Bastida, S. Paria, M. Fagnoni, P. Melchiorre, *Nature* **2016**, *532*, 218–222.
- [84] Z.-Y. Cao, T. Ghosh, P. Melchiorre, *Nat. Commun.* **2018**, *9*, 3274.
- [85] M. Silvi, C. Verrier, Y. P. Rey, L. Buzzetti, P. Melchiorre, *Nat. Chem.* **2017**, *9*, 868–873.
- [86] a) M. Berger, D. Carboni, P. Melchiorre, *Angew. Chem. Int. Ed.* **2021**, *60*, 26373–26377; *Angew. Chem.* **2021**, *133*, 26577–26581; b) C. Verrier, N. Alandini, C. Pezzetta, M. Moliterno, L. Buzzetti, H. B. Hepburn, A. Vega-Peñalosa, M. Silvi, P. Melchiorre, *ACS Catal.* **2018**, *8*, 1062–1066; c) P. Bonilla, Y. P. Rey, C. M. Holden, P. Melchiorre, *Angew. Chem. Int. Ed.* **2018**, *57*, 12819–12823; *Angew. Chem.* **2018**, *130*, 13001–13005.
- [87] D. Mazzarella, G. E. M. Crisenza, P. Melchiorre, *J. Am. Chem. Soc.* **2018**, *140*, 8439–8443.
- [88] a) E. Le Saux, D. Ma, P. Bonilla, C. M. Holden, D. Lustosa, P. Melchiorre, *Angew. Chem. Int. Ed.* **2021**, *60*, 5357–5362; *Angew. Chem.* **2021**, *133*, 5417–5422; b) G. Goti, B. Bieszczad, A. Vega-Peñalosa, P. Melchiorre, *Angew. Chem. Int. Ed.* **2019**, *58*, 1213–1217; *Angew. Chem.* **2019**, *131*, 1226–1230.
- [89] C. Zhu, N. W. J. Ang, T. H. Meyer, Y. Qiu, L. Ackermann, *ACS Cent. Sci.* **2021**, *7*, 415–431.
- [90] T. Shono, Y. Matsumura, H. Hamaguchi, T. Imanishi, K. Yoshida, *Bull. Chem. Soc. Jpn.* **1978**, *51*, 2179–2180.
- [91] T. Chiba, M. Okimoto, H. Nagai, Y. Takata, *J. Org. Chem.* **1979**, *44*, 3519–3523.
- [92] T. Chiba, Y. Takata, *J. Org. Chem.* **1977**, *42*, 23–27.
- [93] N. N. Bui, X. H. Ho, S. Il Mho, H. Y. Jang, *Eur. J. Org. Chem.* **2009**, 5309–5312.
- [94] K. L. Jensen, P. T. Franke, L. T. Nielsen, K. Daasbjerg, K. A. Jørgensen, *Angew. Chem. Int. Ed.* **2010**, *49*, 129–133; *Angew. Chem.* **2010**, *122*, 133–137.
- [95] X. H. Ho, S. Il Mho, H. Kang, H. Y. Jang, *Eur. J. Org. Chem.* **2010**, 4436–4441.
- [96] L. Ackermann, *Acc. Chem. Res.* **2020**, *53*, 84–104.

- [97] N. Fu, L. Li, Q. Yang, S. Luo, *Org. Lett.* **2017**, *19*, 2122–2125.
- [98] a) X. Liu, S. Sun, Z. Meng, H. Lou, L. Liu, *Org. Lett.* **2015**, *17*, 2396–2399;  
b) X. Liu, Z. Meng, C. Li, H. Lou, L. Liu, *Angew. Chem. Int. Ed.* **2015**, *54*,  
6012–6015; *Angew. Chem.* **2015**, *127*, 6110–6113.
- [99] Q. Yang, L. Zhang, C. Ye, S. Luo, L.-Z. Wu, C.-H. Tung, *Angew. Chem. Int. Ed.* **2017**, *56*, 3694–3698; *Angew. Chem.* **2017**, *129*, 3748–3752.
- [100] F. Y. Lu, Y. J. Chen, Y. Chen, X. Ding, Z. Guan, Y. H. He, *Chem. Commun.* **2020**, *56*, 623–626.
- [101] D.-Z. Lin, J.-M. Huang, *Org. Lett.* **2019**, *21*, 5862–5866.
- [102] L. Li, Y. Li, N. Fu, L. Zhang, S. Luo, *Angew. Chem. Int. Ed.* **2020**, *59*,  
14347–14351; *Angew. Chem.* **2020**, *132*, 14453–14457.

---

Manuscript received: March 15, 2022

Accepted manuscript online: June 6, 2022

Version of record online: July 4, 2022